Quantum dots: from theory to applications

Rashid Nazmitdinov

BLTP, JINR, Dubna, Russia

Dubna, 17-22 September, 2018

Outline :

- Introduction: basics
- 2e quantum dot: quantum computer ?
- Quantum dots as building blocks for photovoltaics.

Confining electrons in a semiconductor

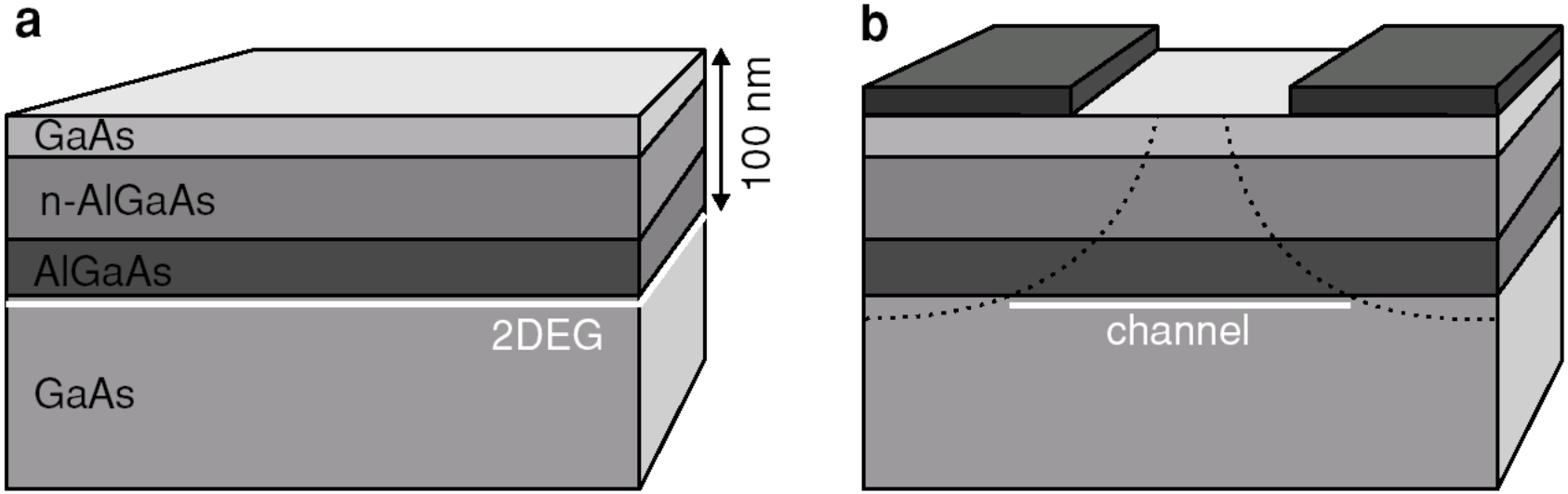

J.M. Elzerman et al.: *Semiconductor Few-Electron Quantum Dots as Spin Qubits*, Lect. Notes Phys. **667**, 25–95 (2005) (Springer, Berlin)

(**a**) Semiconductor heterostructure containing a 2DEG (indicated in *white*) approximately 100nm below the surface, at the interface between GaAs and AlGaAs. The electrons in the 2DEG result from Si donors in the n-AlGaAs layer. (The thickness of the diferent layers is not to scale.)
(**b**) By applying negative voltages to the metal electrodes on the surface of the heterostructure, the underlying 2DEG can be locally depleted. In this way, electrons can be confned to one or even zero dimensions

Spin-orbit in a semiconductor

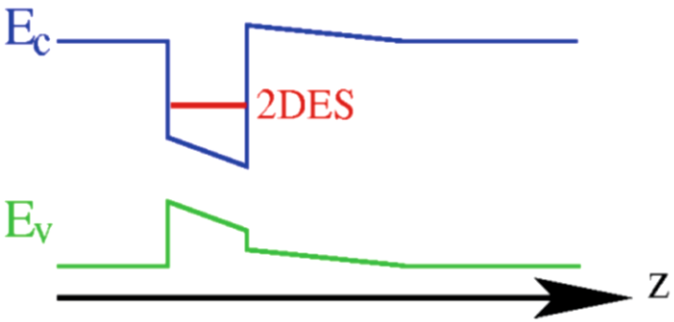

$$\mathbf{B} = [\mathbf{E} \times \tfrac{\mathbf{v}}{c}]; \quad \mathbf{E} = \tfrac{1}{e}\vec{\nabla} V(\mathbf{r})$$

$$\hat{\mu} = \frac{e\hbar}{2mc}\hat{\sigma}; \quad \frac{\mathbf{v}}{c} = -\frac{i\hbar}{mc}\hat{\nabla}$$

$$\mu\mathbf{B} = -\frac{i\hbar^2}{2m^2c^2}\hat{\sigma}[\vec{\nabla} V \times \hat{\nabla}]$$

$$\vec{\nabla} V = \frac{\hat{r}}{r}\frac{\partial V}{\partial r}$$

$$\mu\mathbf{B} = -\frac{i\hbar^2}{2m^2c^2}\frac{\partial V}{\partial r}\frac{\hat{r}}{r}[\hat{\nabla} \times \hat{\sigma}]$$

$$\mathcal{H} = T + V(\mathbf{r}) + \frac{\hbar}{m}\alpha\hat{z}[\hat{p} \times \hat{\sigma}]_z$$

$$[\hat{\boldsymbol{p}} \times \hat{\sigma}]_z = \hat{\boldsymbol{p}}_x\hat{\sigma}_y - \hat{\boldsymbol{p}}_y\hat{\sigma}_x$$

$$m \Rightarrow m*$$

$$\alpha = \frac{1}{2m*c^2 z}\left(\frac{\partial V}{\partial r}\right)_z$$

Spin-orbit coupling:

Relativistic Particle Physics

$\hookrightarrow$ decoupling particles and antiparticles

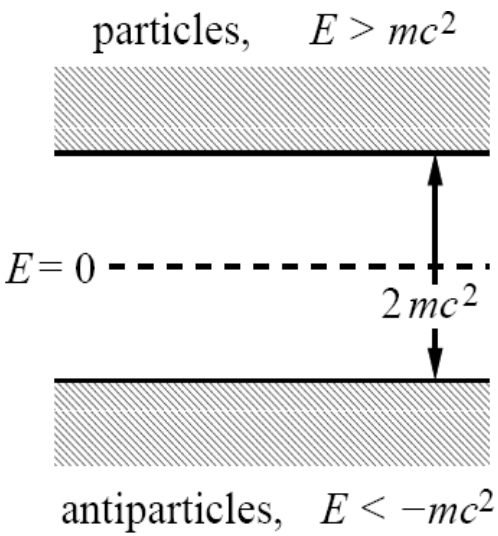

$\Rightarrow$ **Pauli Equation**

$$H = \frac{p^2}{2m} + V$$

kinetic and potential energy

$$+ \frac{g}{2}\mu_{\mathrm{B}}\,\boldsymbol{\sigma}\cdot\mathbf{B}$$

Zeeman term

$$+ \frac{\hbar}{4m_0^2c^2}(\nabla V)\times\mathbf{p}\cdot\boldsymbol{\sigma}$$

Pauli spin-orbit coupling

Spin-orbit coupling:

- spin–orbit coupling: relativistic correction to electron's kinetic energy; motional + spin states interdependent

$$H_{\rm so} = \frac{1}{2m_0}\left[\vec{p}\times\hbar\vec{\nabla}\left(\frac{V_{\rm ext}}{2m_0c^2}\right)\right]\cdot\vec{\sigma} \quad \text{in vacuum}$$

- in solids: electron states similar to those in vacuum, but parameters (e.g., mass, or strength of spin–orbit coupling) changed from that for free electrons
  - in the conduction band of III–V semiconductors (InAs):

$$H_{\rm so} = \frac{1}{2m_*}\left[\vec{p}\times\hbar\vec{\nabla}\left(\frac{V_{\rm ext}}{2E_{\rm g}}\right)\right]\cdot\vec{\sigma} \quad \text{(for small band gap } E_{\rm g}\text{)}$$

Spectral Problem of Rashba Hamiltonian

- Rashba Hamiltonian of **infinite 2DEG**: Kinetic energy + SO coupling

$$\hat{H}_{2D} = \frac{\hat{p}_x^2 + \hat{p}_y^2}{2m} + \frac{\alpha}{\hbar}(\hat{p}_y\hat{\sigma}_x - \hat{p}_x\hat{\sigma}_y) \Rightarrow [\hat{H}_{2D}, \hat{\vec{p}}] = 0$$

- Since Hamiltonian commutes with the 2D momentum operator, we can classify its eigenvectors and eigenvalues with wave numbers k_x, k_y :

$$\begin{pmatrix} \frac{\hbar^2}{2m^*}(k_x^2 + k_y^2) & i\alpha k_x + \alpha k_y \\ -i\alpha k_x + \alpha k_y & \frac{\hbar^2}{2m^*}(k_x^2 + k_y^2) \end{pmatrix} \psi_\pm = E_\pm \psi_\pm$$

$$E_\pm = \frac{\hbar^2 k^2}{2m} \pm \alpha k, \quad k \equiv |\vec{k}|$$

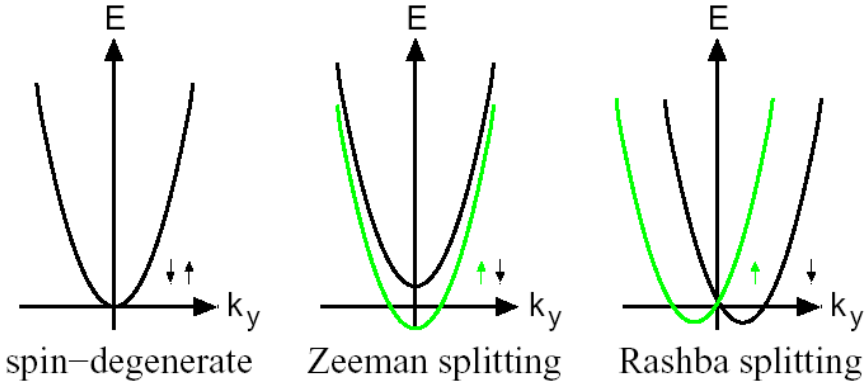

Spin splitting: mechanisms

Spin degeneracy

spatial inversion symmetry:

$$E(\mathbf{k},\uparrow) = E(-\mathbf{k},\uparrow)$$

time inversion symmetry (Kramers):

$$E(\mathbf{k},\uparrow) = E(-\mathbf{k},\downarrow)$$

$$\Bigg\} \quad E(\mathbf{k},\uparrow) = E(\mathbf{k},\downarrow)$$

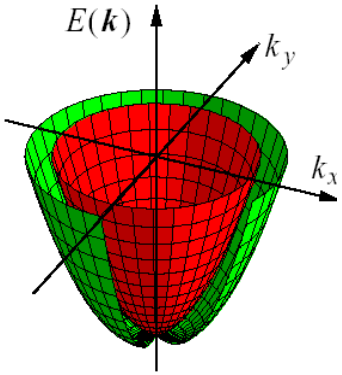

Inversion asymmetry $\Rightarrow$ $\boxed{E(\mathbf{k},\uparrow) \neq E(\mathbf{k},\downarrow)}$

$\Rightarrow$ two energy surfaces $E_{\pm}(\mathbf{k})$

Caused by:

spin-orbit interaction

$+\begin{cases} \text{bulk inversion asymmetry, e.g., zinc blende structure} \\ \text{structure inversion asymmetry, e.g., gate} \end{cases}$

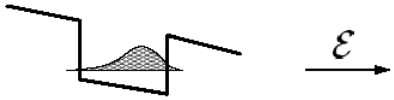

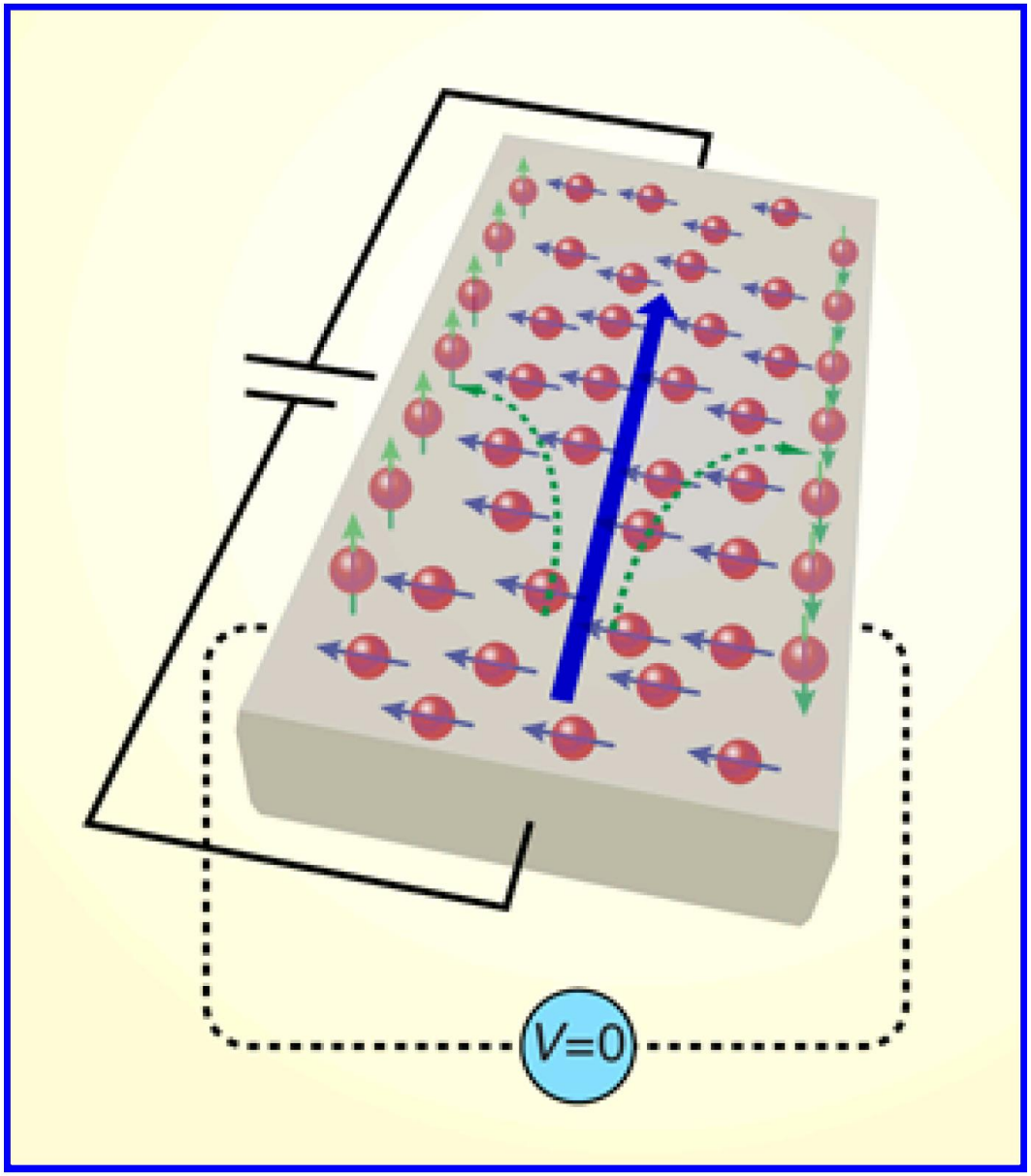

Figure 1: Electrically-injected electrons become spin polarized through two different mechanisms during nominally "simple" transport in semiconductors. Electrons can experience anisotropic spin scattering from impurities in the presence of spin-orbit coupling, producing the spin Hall effect where "up" and "down" spins (green arrows) accumulate at opposite edges of the channel. In addition, symmetry-related spin-orbit fields can produce a homogeneous electron spin polarization throughout the channel (blue arrows).

Electronics: old concepts

- conventional electronics uses only electron's charge

e.g., bipolar transistor

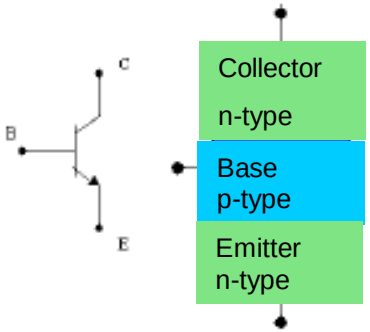

or field–effect transistor

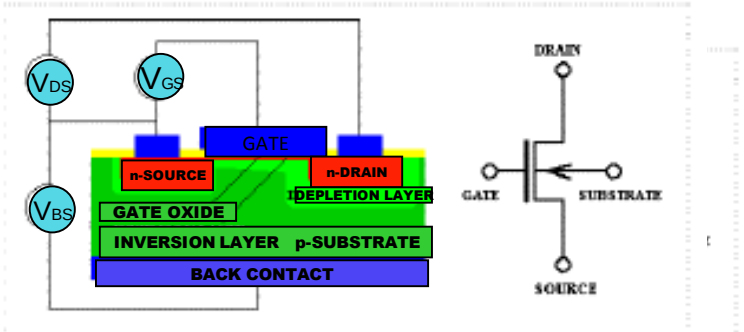

Spintronics : charge and spin carriers

- higher level of device integration
- faster data manipulation
- lower power consumption

Novel devices based on laws of quantum mechanics !

I.Zutic, J.Fabian and S. Das Sarma, Rev.Mod. Phys. **76**, 323 (2004).

D.D. Awschalom and M.E. Flatte, Nature Phys. **3**, 153 (2007).

magnetoelectronics

- electron = charge and spin carrier: spin(elec)tronics

Ideal magnetoresistance.

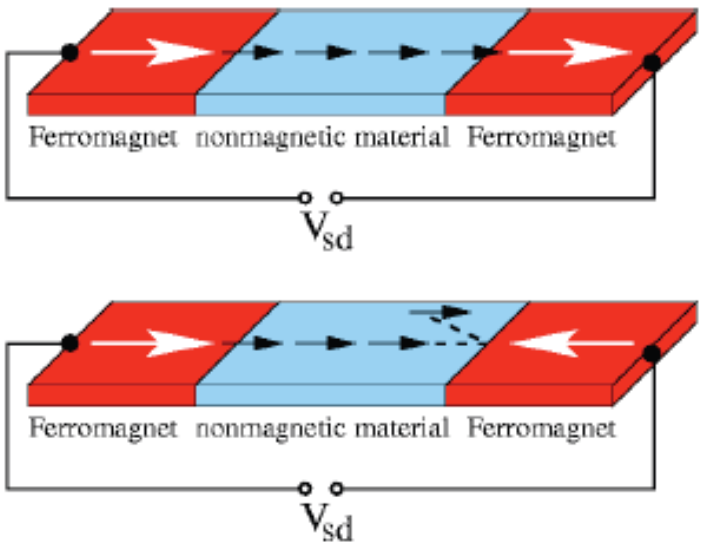

Two half-metallic ferromagnets, having only majority type conduction electrons, are connected in series with nonmagnetic conductor between them. When their magnetizations are parallel (upper panel), majority electrons injected from one electrode are majority electrons in the second electrode, and current is finite for finite source-drain voltage. In the antiparallel configuration (lower panel), electrons injected from the left electrode cannot enter the second electrode because no minority electrons are allowed to exist there.

data storage technology

spintronics:

Datta and Das spin-transistor
Appl.Phys.Lett. **56,** 665 (1990)

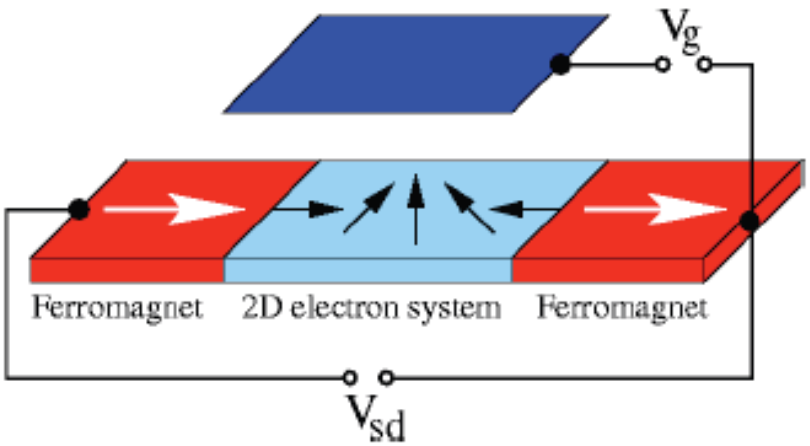

Electrons ballistically pass through a channel and their spin precession angle is controlled by

$$\Delta\theta = 2m^*\alpha L/\hbar^2$$

- **Spin-orbit coupling in nonmagnetic 2D electron system induces a precession of spin (indicated as short arrows) for electrons propagating between ferromagnetic contacts. The length scale on which a full spin rotation occurs is tunable by a gate voltage (Vg). Hence, the spin precession of electrons injected into the 2D electron system by a magnetic (polarizer) electrode can be adjusted such that they become either majority or minority electrons in the second (analyser) electrode. Such a field-effect switch works without charge accumulation in the semiconductor.**

QDs created in thin film semiconductor heterostructures

With the use of epitaxial deposition techniques (like molecular beam epitaxy) it is possible to grow semiconductor crystals in coherent layers, a few lattice constant thick, and create multilayer semiconductor heterostructures.

By sandwiching a 10 nm thickness of GaAs between AlGaAs (insulator) layers, one confines electrons in a GaAs 'quantum well'.

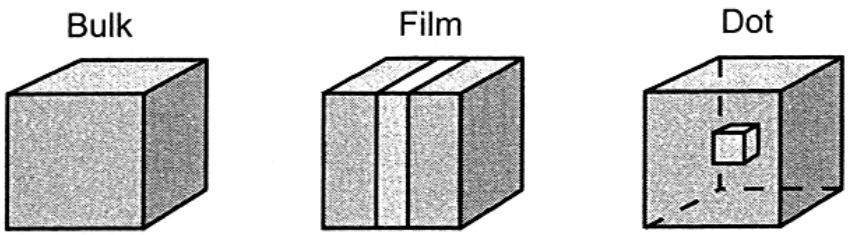

Reduction of the remaining 2D ‘infinite’ extension of the quantum well, i.e. lateral confinement, leads to carrier confinement in all three dimensions and creation of a QD.

Basics

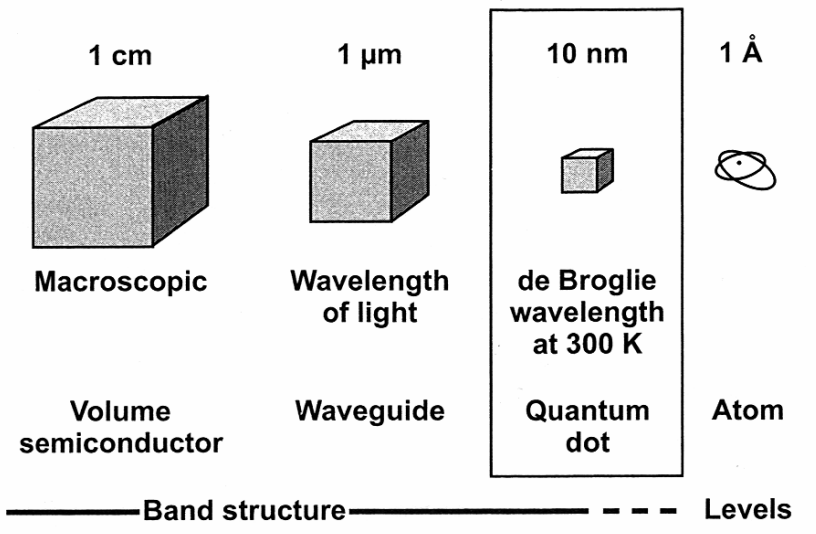

If the carrier motion in a solid is limited in a layer of a thickness of the order of the carrier de Broglie wavelength (λ), one will observe effects of size quantization.

$$\lambda = \frac{h}{p} = \frac{h}{\sqrt{3m_{eff}kT}} = \frac{1.22\,\text{nm}}{\sqrt{E_{kin}/[\text{eV}]}}$$

Quantum dots (QD) are small boxes (2 – 10 nm on a side, corresponding to 10 to 50 atoms in diameter), contained in semiconductor, and holding a number of electrons.

At 10 nm in diameter, nearly 100000 quantum dots can be fit within the width of a human thumb.

The confinement can be due to electrostatic potentials (generated by external elctrodes), due to the presence of interface between different semiconductors (SAQD), due to the presence of the semiconductor surface (a semiconductor nanocrystal).

Electrostatic DQs

M.A.Reed et al, PRL **60**, 535 (1988)

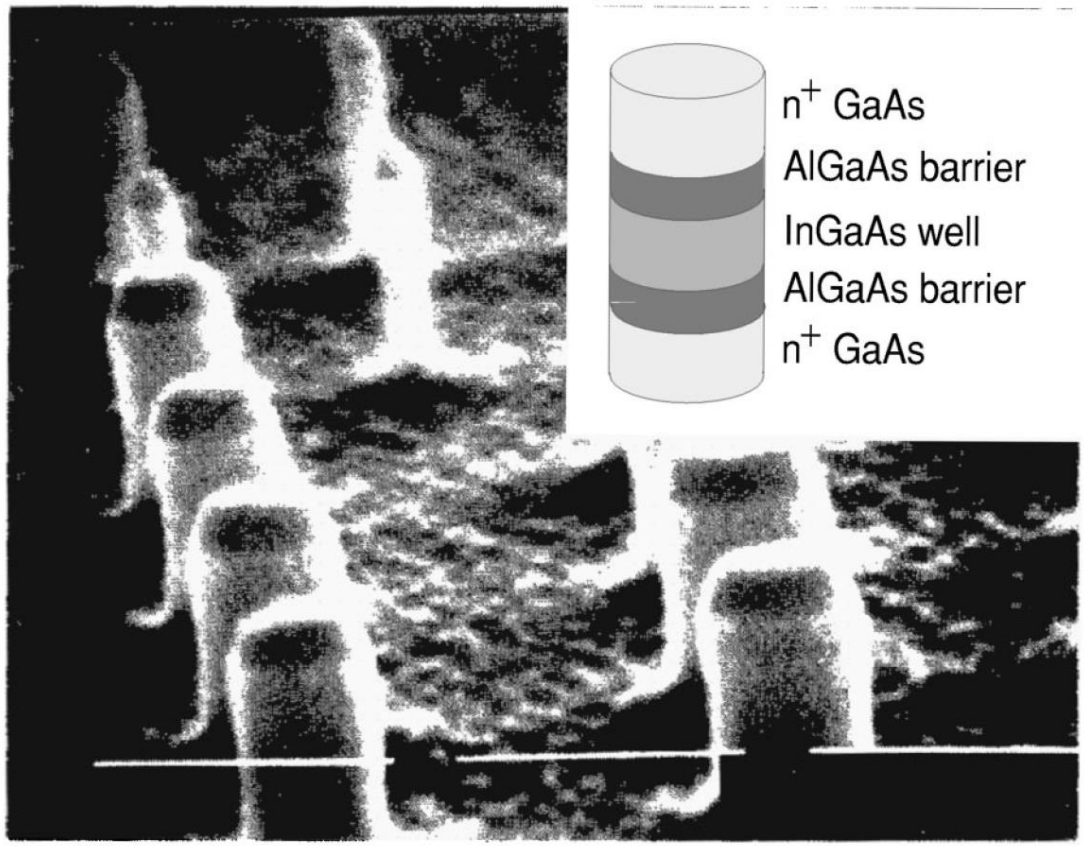

A scanning electron micrograph of various size GaAs nanostructures containing quantum dots. The dark regions on top of the column is the electron-beam defined Ohmic contact and etch mask. The horizontal bars are 0.5 μm.

Electrostatic DQs

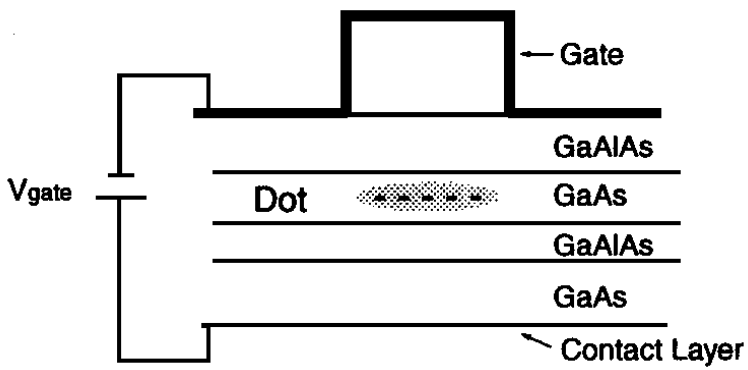

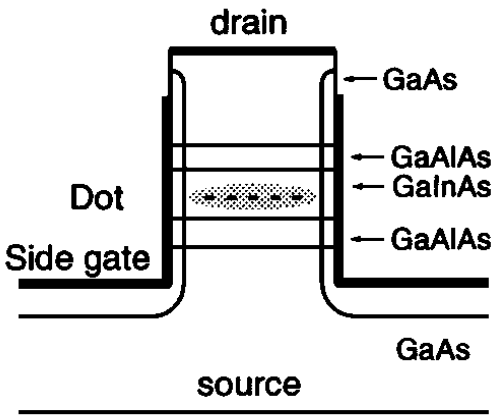

Schematic illustration of typical electrostatic DQs. Left-hand side: capped dot; right-hand side: pillar dot. The capped dot can be made either from a quantum well (as shown) or from a heterojunction.

- By sandwiching a 10 nm thickness of GaAs between AlGaAs (insulator) layers, one confines electrons in a GaAs 'quantum well'. By placing electrostatic gates on the surface of the wafer, we can laterally confine this 2D electron gas and create a quantum dot

- For the typical voltage ~ 1V applied to the gate (top plate), the confining potential is some eV deep which is large compared to the few meV of the confining frequency. Hence, the electron wave function is localized close to the minimum of the well which always can be approximated by a parabolic potential.

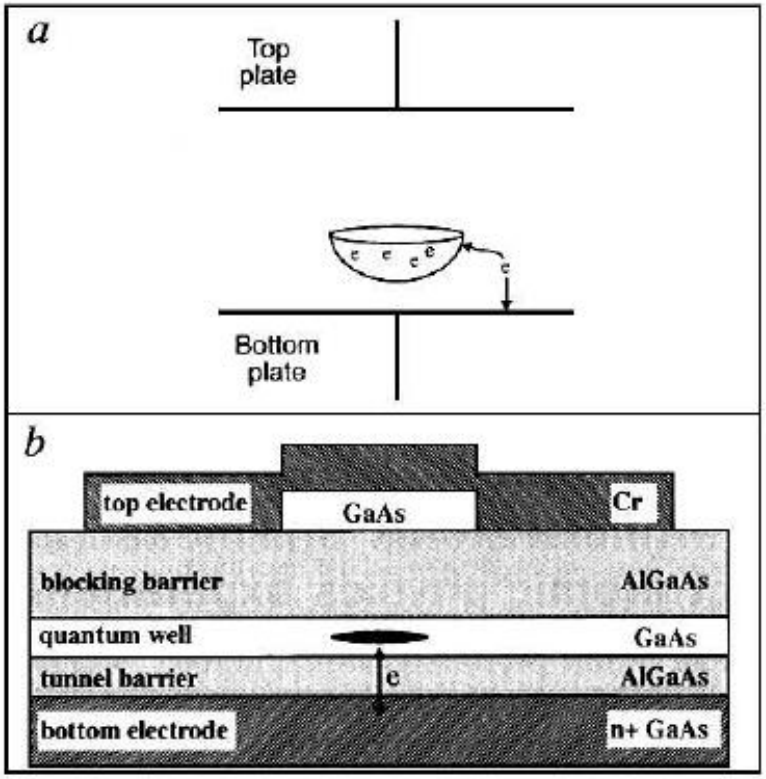

FIR spectroscopy

Sikorski and Merkt, PRL **62** (1989) 2164 - The first direct observation of resonance transitions between discrete states of QDs on InSb.

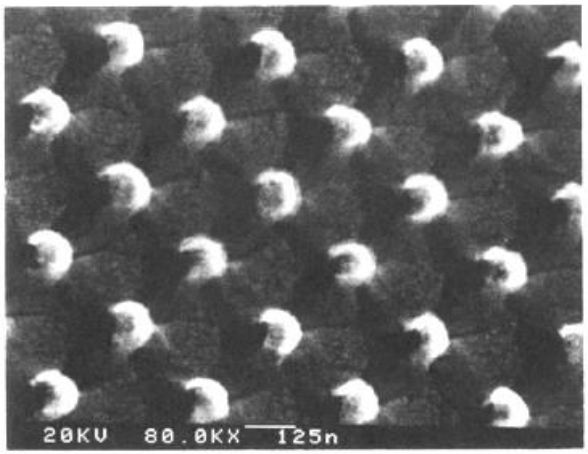

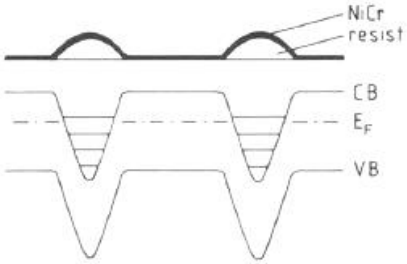

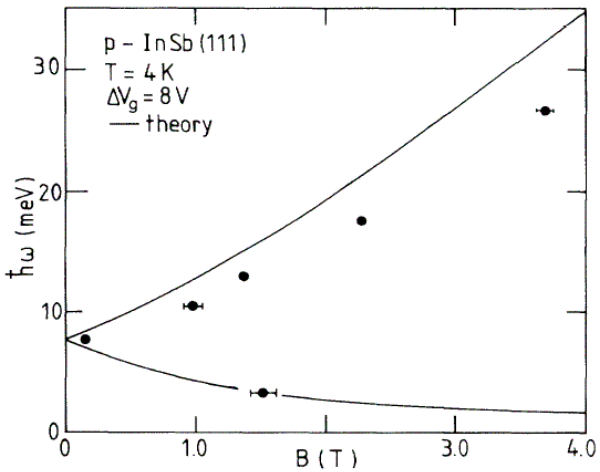

<u>Left</u>: Scanning electron micrograph of arrays of QDs on InSb and the schematic sketch of the band structure across the dots.
<u>Right</u>: Experimental resonance positions (bullets) together with theoretical curves calculated from $\omega_{\pm} = (\omega_0^2 + \omega_L^2)^{1/2} \pm \omega_L$.

Single-electron quantum dot

The Hamiltonian

$$H = \frac{1}{2m^*}\left(\vec{p} - \frac{e}{c}\vec{A}\right)^2 + \frac{m^*}{2}\omega_0^2(x^2 + y^2)$$

Using the symmetric gauge $\vec{A} = \frac{1}{2}[\vec{B} \times \vec{r}]$ with $\vec{B} = (0,0,B)$, it follows

$$H = \frac{p_x^2 + p_y^2}{2m^*} + \frac{m^*}{2}\Omega_0^2(x^2 + y^2) - \omega_L l_z$$

where $\omega_L = eB/2m^*c$ is a Larmor frequency and $\Omega_0 = [\omega_0^2 + \omega_L^2]^{1/2}$.

The problem was solved more than 90 years ago (Fock, 1928; Darwin 1930).
The so called Fock-Darwin levels are

$$E_{n.m} = \hbar\Omega_0(2n + |m| + 1) \pm \hbar\omega_L m$$

where n and m are the radial and magnetic quantum numbers

FIR spectroscopy

Sikorski and Merkt, PRL **62** (1989) 2164 - The first direct observation of resonance transitions between discrete states of QDs on InSb.

The problem was solved more than 90 years ago (Fock 1928, Darwin 1930). The so-called Fock-Darwin energy levels are

$$H = \frac{1}{2m^*}(\mathbf{p} - e\mathbf{A})^2 + \frac{1}{2}m^*\omega_0^2(x^2 + y^2).$$

$$\mathbf{A} = \frac{1}{2}\mathbf{B}\times\mathbf{r}, \;\; \mathbf{B} = (0,0,B),$$

$$H = \frac{p_\rho^2}{2m^*} + \frac{l_z^2}{2m^*\rho^2} + \frac{1}{2}m^*\Omega^2\rho^2 - \omega_L l_z\,,$$

where $\omega_L = eB/2m^*$ is the Larmor frequency and

$$E_{nm} = \hbar\Omega(2n + |m| + 1) - \hbar\omega_L m,$$

$$\Omega^2 = \omega_0^2 + \omega_L^2\,.$$

$$\boxed{\omega_\pm = (\omega_0^2 + \omega_L^2)^{1/2} \pm \omega_L\,.}$$

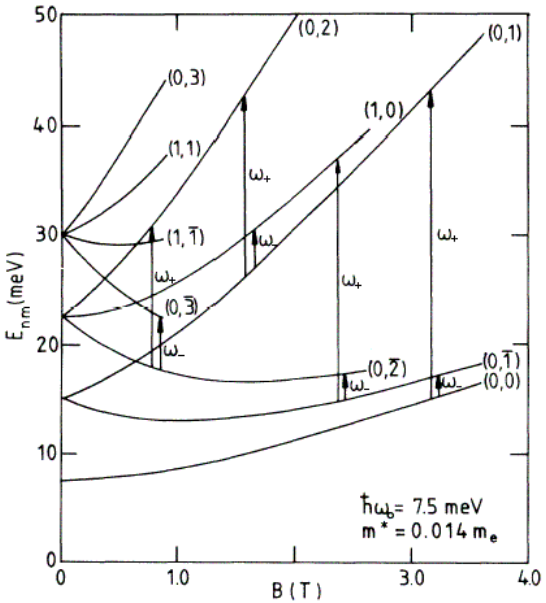

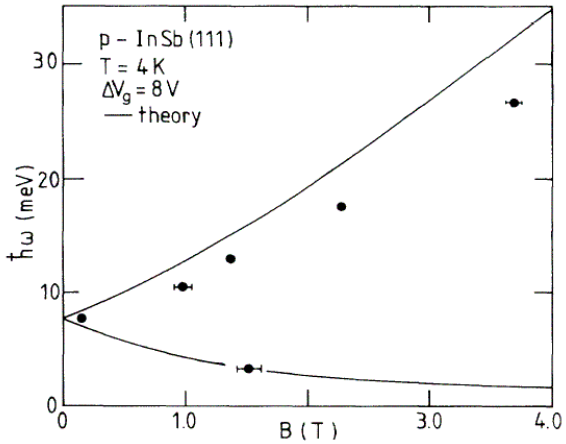

The Kohn theorem

<u>The Kohn theorem</u> - In a parabolic confining potential the centre-of-mass (CM) and relative (rel) motion decouple.

For a *N*-electron QD:

$$H = \frac{1}{2M}\left(\mathbf{P} + Q\mathbf{A}\right)^2 + \frac{1}{2}M\omega_0^2 R^2 + H_{rel}\,,$$

where $\mathbf{P} = \sum_{i=1}^{N}\mathbf{p}_i$, $\mathbf{R} = \sum_{i=1}^{N}\mathbf{r}_i/N$, $Q = Ne$, $M = Nm^*$.

Since $Q/M = e/m^*$, the CM energy is identical to the single-electron energy E_{nm}.

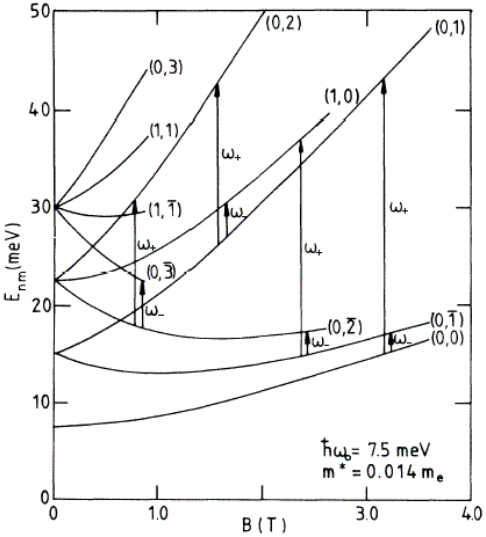

<u>The generalized Kohn theorem</u> – The far-infrared (FIR) absorption spectra are independent on the number of electrons.

$$d_{nm,n'm'} = \langle nm | r\,\mathrm{e}^{\mathrm{i}\varphi} | n'm' \rangle,$$

$$\Delta m = \pm 1, \quad \Delta n = 0,1.$$

$$\Delta E_{\pm} = \hbar\omega_{\pm} = \hbar\Omega \pm \hbar\omega_L\,,$$

Lateral and vertical quantum dots

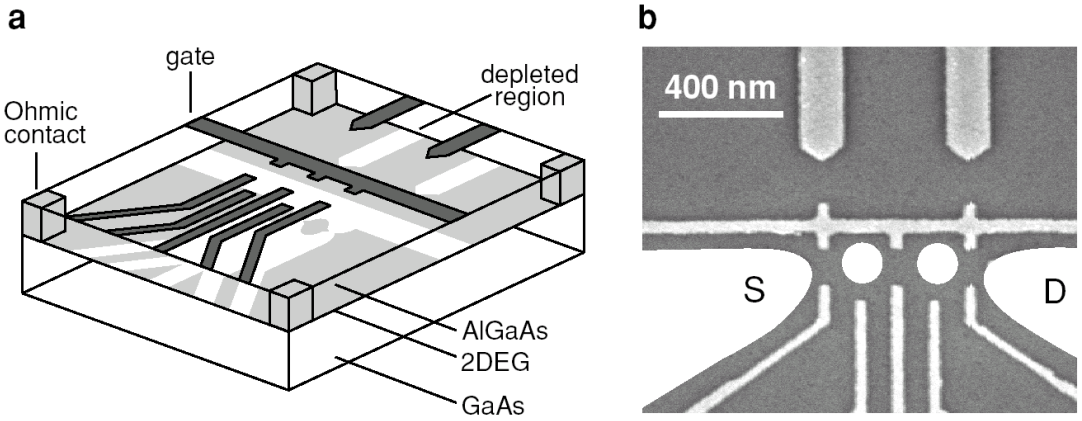

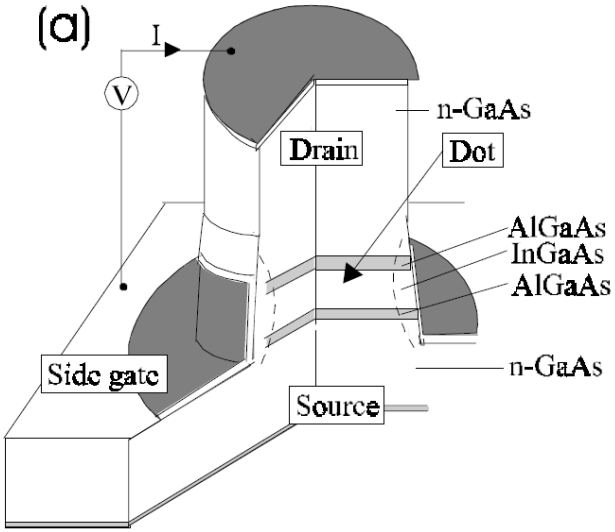

(**a**) Schematic view of a device. Negative voltages applied to metal gate electrodes (*dark gray*) lead to depleted regions (*white*) in the 2DEG (*light gray*). Ohmic contacts (*light gray* columns) enable bonding wires (not shown) to make electrical contact to the 2DEG reservoirs.
(**b**) Scanning electron microscope image of an actual device, showing the gate electrodes (*light gray*) on top of the surface (*dark gray*). The two *white dots* indicate two quantum dots, connected via tunable tunnel barriers to a source (S) and drain (D) reservoir, indicated in *white*.
The two *upper* gates can be used to create two quantum point contacts, in order to detect changes in the number of electrons on the dot

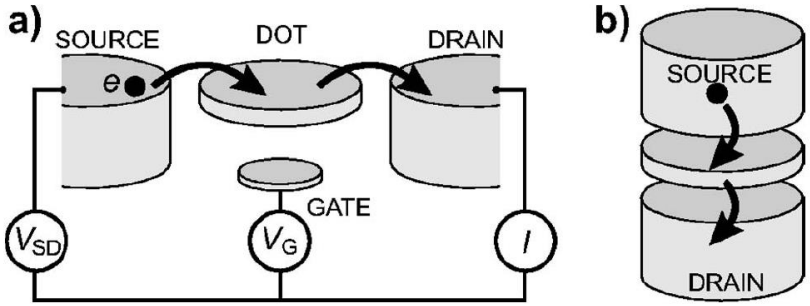

Conductance

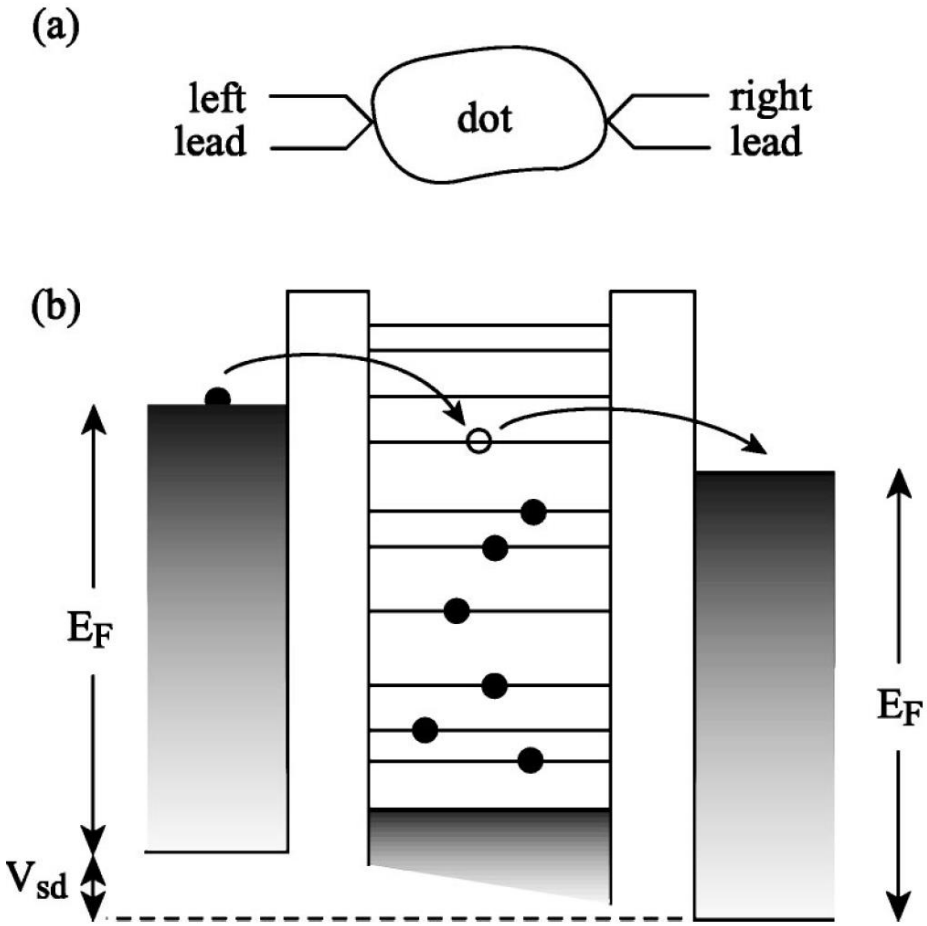

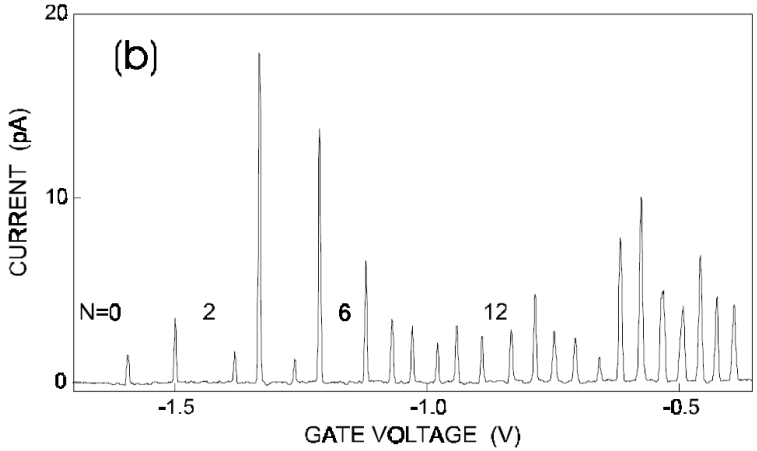

Coulomb blockade:

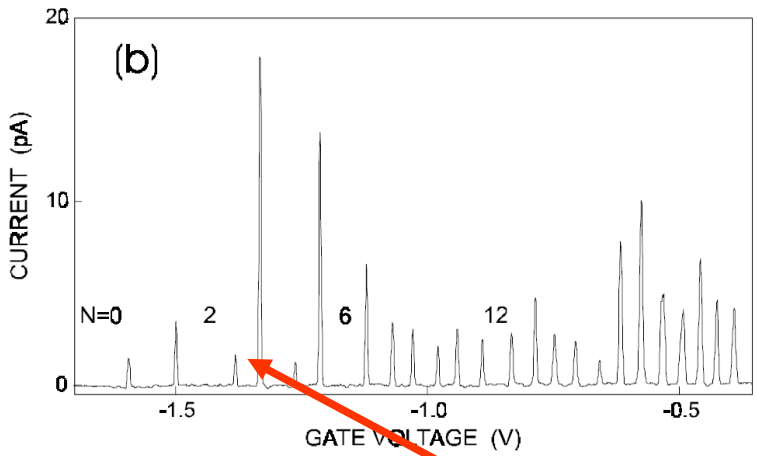

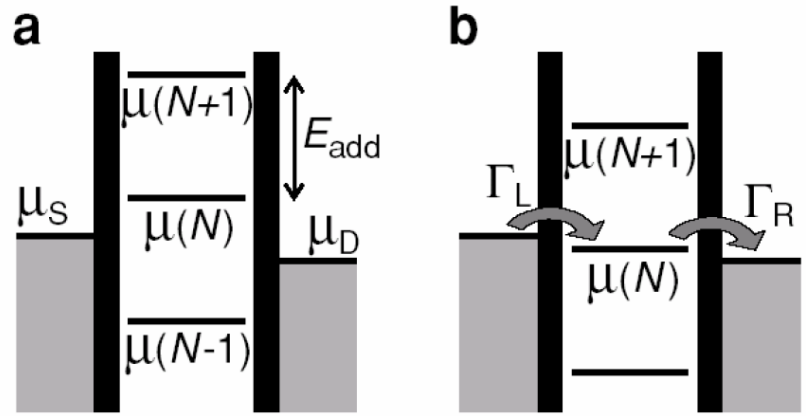

$$\mu(N) = U(N) - U(N-1)$$

$$E_{add} = \mu(N) - \mu(N-1)$$

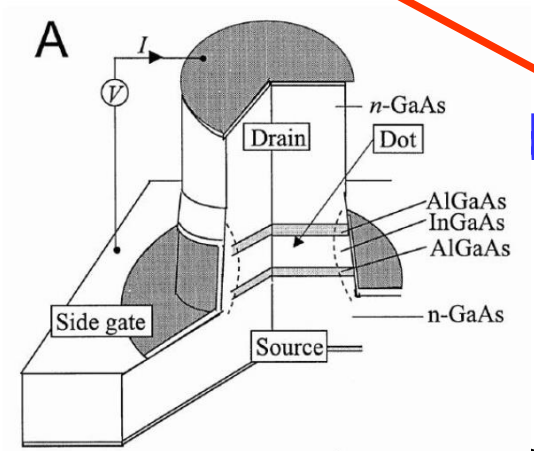

Con lel: classical component

$U(N$

$E_{add} = \varepsilon_N - \varepsilon_{N-1} + e^2/C \sim e^2/C$

macroscopic energy is not able to explain the add.energies

Shell structure in quantum dot

Heiss&Nazmitdinov, *Phys.Lett.**A222** (1996) 309*

$$H = \sum_{i=1}^{N} h_i$$

$$N = n_+ + n_-$$

$$h = \frac{1}{2m^*}(\vec{p} - \frac{e}{c}\vec{A})^2 + \frac{m^*}{2}(\omega_x^2 x^2 + \omega_y^2 y^2) + \mu^* \sigma_z B.$$

$\vec{A} = [\vec{r} \times \vec{B}]/2$, $\vec{B} = (0, 0, B)$ and σ_z is the Pauli matrix.

$$\mu^* = 0.5\mu_B \qquad \mu_B = |e|\hbar/2m_e c \qquad \omega_L = eB/2m^* c$$

$$E^0_{n_+ n_-} = \hbar\Omega_+(n_+ + 1/2) + \hbar\Omega_-(n_- + 1/2)$$

$$\Omega_\pm^2 = \frac{1}{2}(\omega_x^2 + \omega_y^2 + 4\omega_L^2 \pm \sqrt{(\omega_x^2 - \omega_y^2)^2 + 8\omega_L^2(\omega_x^2 + \omega_y^2) + 16\omega_L^4})$$

$$E_{n_+ n_-} = E^0_{n_+ n_-} \pm 1/2\mu_B B$$

$$\delta < H - \lambda\omega_x\omega_y >= 0$$

$$\omega_x \omega_y = const$$

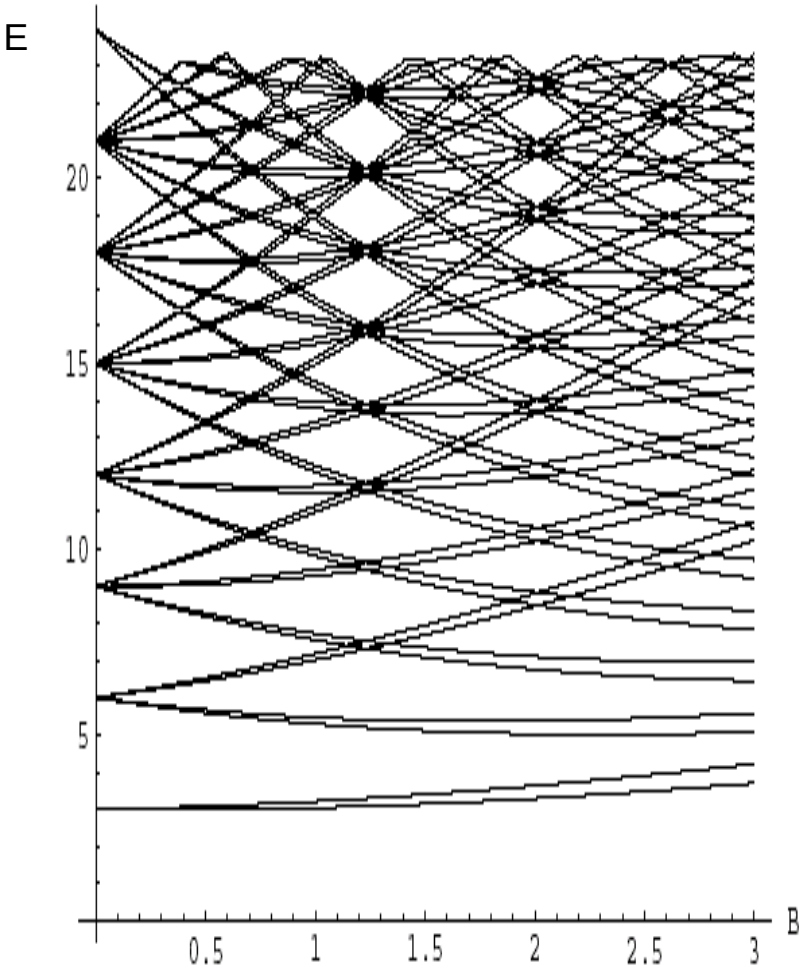

Shell effects in QD

*S.Tarucha et al, Phys. Rev. Lett. **77**, 3613 (1996).*

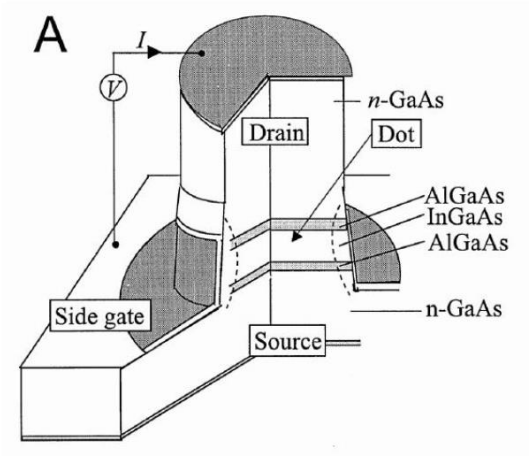

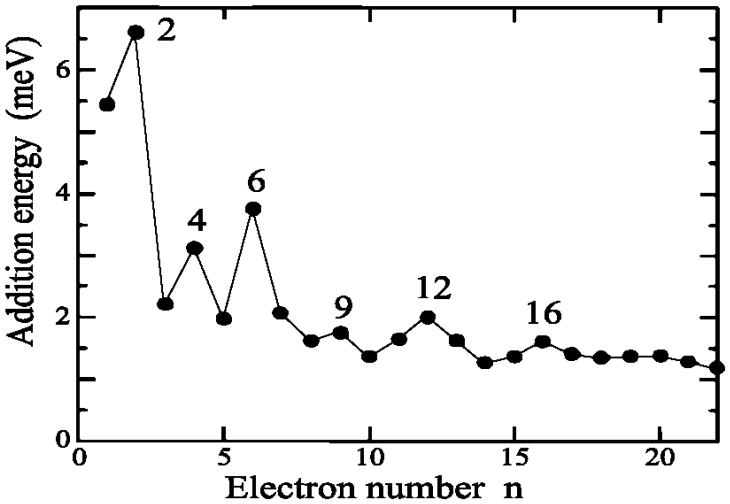

$$H = \sum_i^N h_i$$

$$h = \frac{p^2}{2m^*} + \frac{m^*}{2}\left[\omega_0^2\rho^2 + \omega_z^2 z^2\right]$$

$$\omega_z \geq 1.5\omega_0$$

$$\mu(N) = U(N) - U(N-1)$$

$$E_{add} = \mu(N) - \mu(N-1)$$

$$A = (N_{sh}+1)(N_{sh}+2)$$

=2,6,12..(N_{sh} =0,1,2..)

Shell structure of a circular symmetric shape.

Shell structure

Heiss&Nazmitdinov, Phys. Lett. A**222**, 309 (1996)

- B = 0 the magic numbers (including spin) turn out to to be the usual sequence of the two-dimensional isotropic oscillator, $\omega_x=\omega_y$, that is 2, 6, 12, 20, ...

- B ≈ 1.23 we find a new shell structure as if the confining potential would be a deformed harmonic oscillator without magnetic field. The magic numbers are 2, 4, 8, 12, 18, 24, . . . which are just the numbers obtained from the two-dimensional oscillator with $\omega_+ = 2\,\omega_-$.

- B ≈ 2.01 the magic numbers 2, 4, 6, 10, 14, 18, 24, . . . which corresponds to $\omega_+ = 3\,\omega_-$.

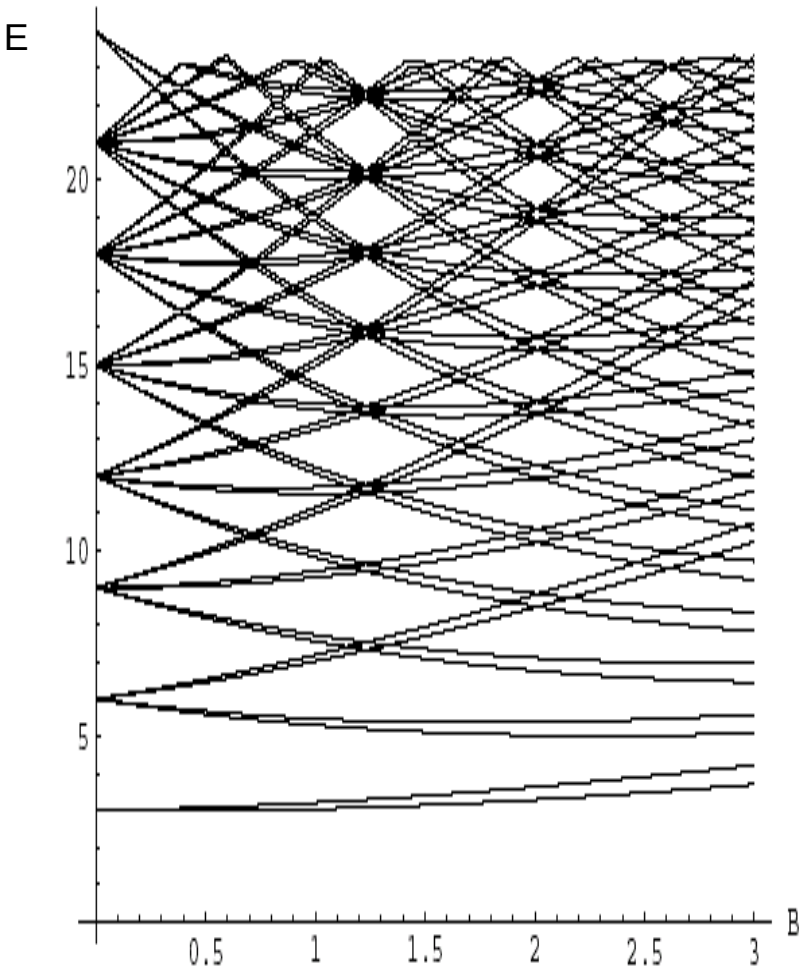

Models

The standard theoretical model is based on a number of approximations:

- The underlying lattice structure is taken into account in effective mass approximation: $m_e \Rightarrow m^*$.
- The confining potential is parabolic.
- The electrons interact via a screened Coulomb interaction.

The Hamiltonian for *N* electrons interacting in a QD in a magnetic field *B*, perpendicular to the dot plane reads:

$$H = \sum_{n=1}^{N}\left[\frac{1}{2m^*}\left(\mathbf{p}_i - e\mathbf{A}_i\right)^2 + \frac{1}{2}m^*\omega_0^2 r_i^2\right] + \frac{e^2}{4\pi\varepsilon_0\varepsilon_r}\sum_{i=1}^{N}\sum_{j>i}^{1,N}\frac{1}{r_{ij}} + g^*\mu_B B S_z ,$$

where e, m^*, ε_0 and ε_r and the unit charge, effective electron mass, vacuum and relative dielectric constant of a semiconductor, respectively.

J.L.Birman, R.G.N., V.I.Yukalov, Phys.Rep.**526**, 1 (2013)

Two-electron quantum dot

The Hamiltonian for the axially symmetric ($\omega_x = \omega_y \equiv \omega_0$) two-electron quantum dot in magnetic field reads

$$
\begin{aligned}
H &= H_0 + H_C + H_Z \\
H_0 &= \sum_{j=1}^{2} \left\{ \frac{1}{2m^*} (\mathbf{p}_j - \frac{e}{c}\mathbf{A}_j)^2 + \frac{m^*}{2} \left[\omega_0^2 (x_j^2 + y_j^2) + \omega_z^2 z_j^2 \right] \right\} \\
H_C &= \frac{\alpha}{|\mathbf{r}_1 - \mathbf{r}_2|}, \qquad H_Z = g^* \mu_B (\mathbf{s}_1 + \mathbf{s}_2) \cdot \mathbf{B}
\end{aligned}
$$

$$
\alpha = \frac{e^2}{4\pi\varepsilon_0\varepsilon_r}, \qquad \mu_B = \frac{e\hbar}{2m_e c}
$$

two-electron states

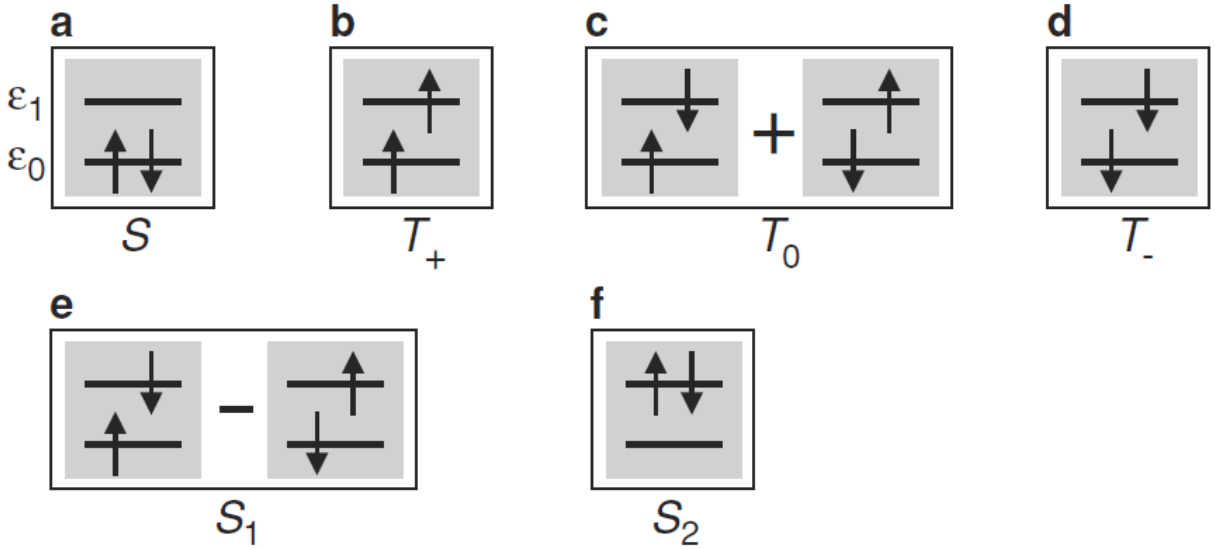

Fig. 9. Schematic energy diagrams depicting the spin states of two electrons occupying two spin degenerate single-particle levels (ε_0 and ε_1). (**a**) Spin singlet, which is the ground state at zero magnetic field. (**b**)–(**d**) Lowest three spin triplet states, T_+, T_0 and T_-, which have total spin $S = 1$ and quantum number $m_s = +1$, 0 and -1, respectively. In finite magnetic field, the triplet states are split by the Zeeman energy. (**e**) Excited spin singlet state, S_1, which has an energy J compared to triplet state T_0. (**f**) Highest excited spin singlet state, S_2

Ground-state transitions in a magnetic field

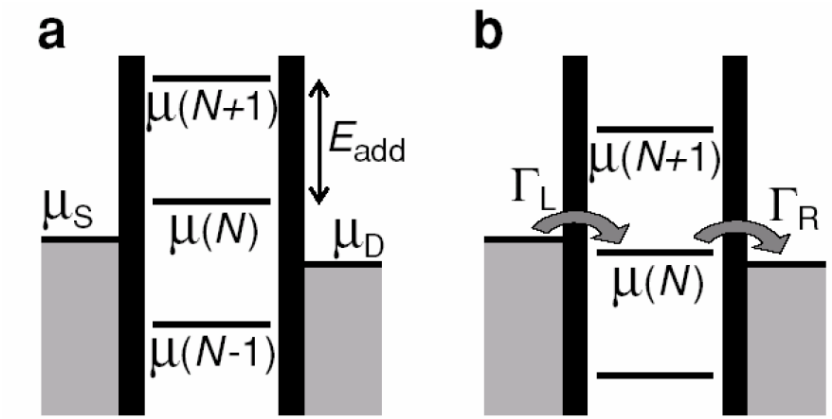

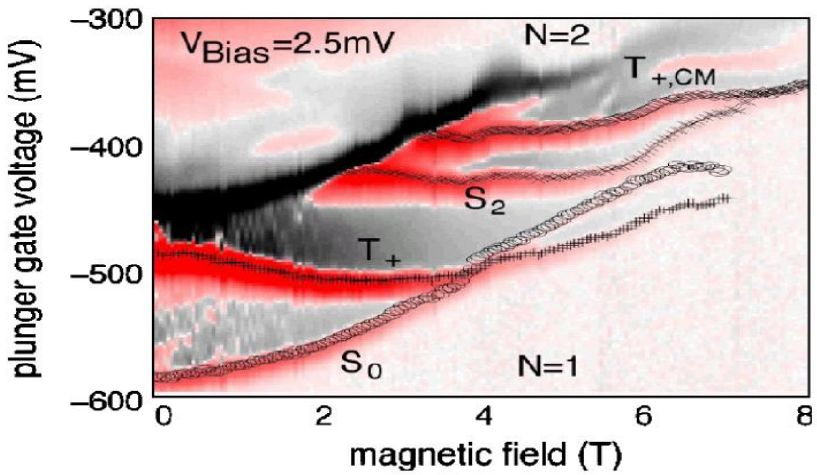

Ellenberger, et al., *PRL* ***96*** *(2006)126806*

FIG. 2 (color online). Differentiated current dI/dV_{pg} at $V_{bias} = 2.5$ mV. Gray striped regions (red online) marked by symbols correspond to positive (peaks) dI/dV_{pg}. The dark black region (also black online) corresponds to negative dI/dV_{pg}.

2eQD in a magnetic field

Nazmitdinov&Simonovic, *PRB**76** (2007)193306*

$$\mu(N) = E_{tot}(N) - E_{tot}(N-1)$$

$$\Delta\mu(N) = \mu(N+1) - \mu(N-1)$$

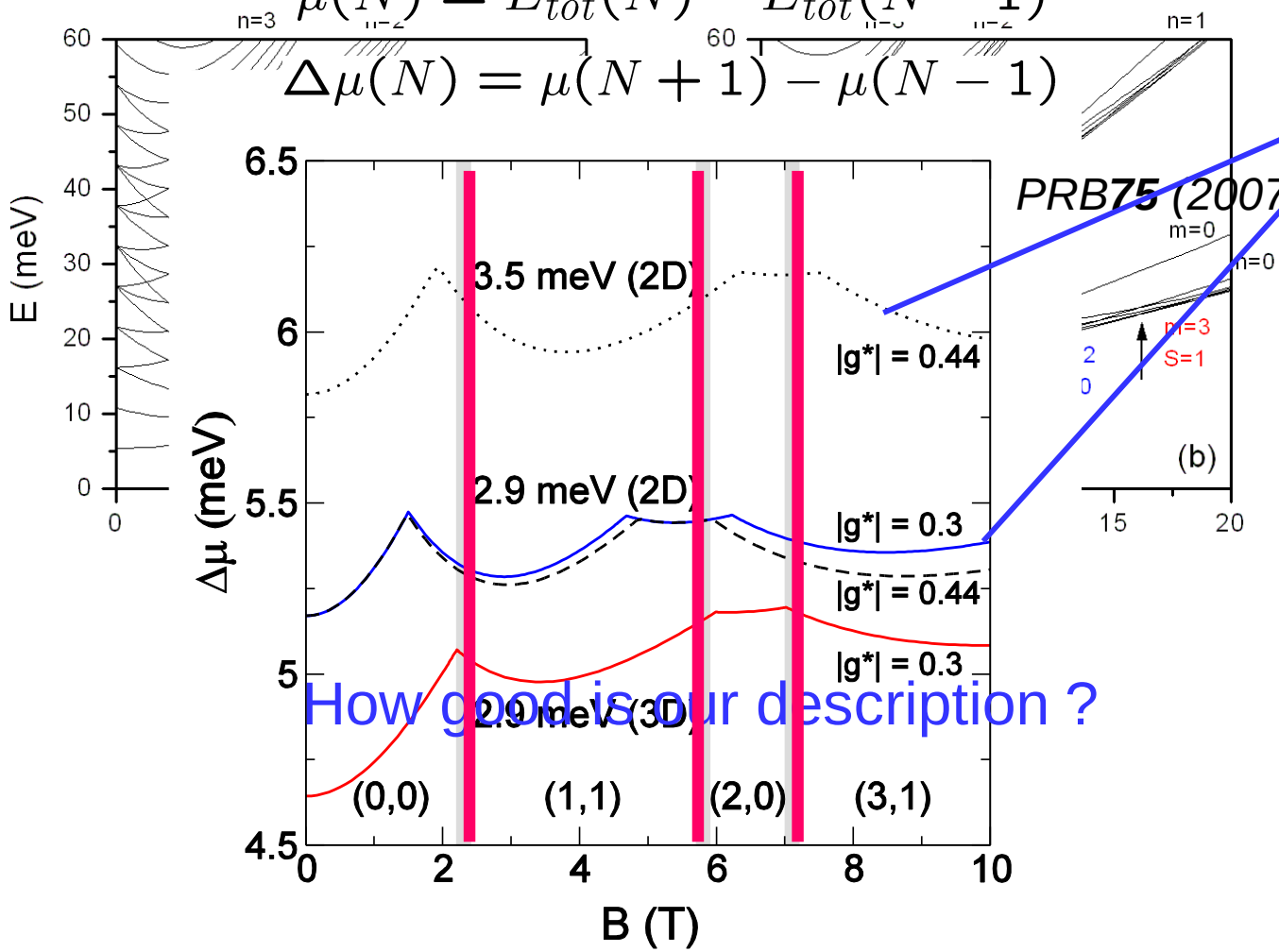

Nishi et al

*PRB**75** (2007) 121301(R)*

How good is our description ?

Spin qubit (basic idea)

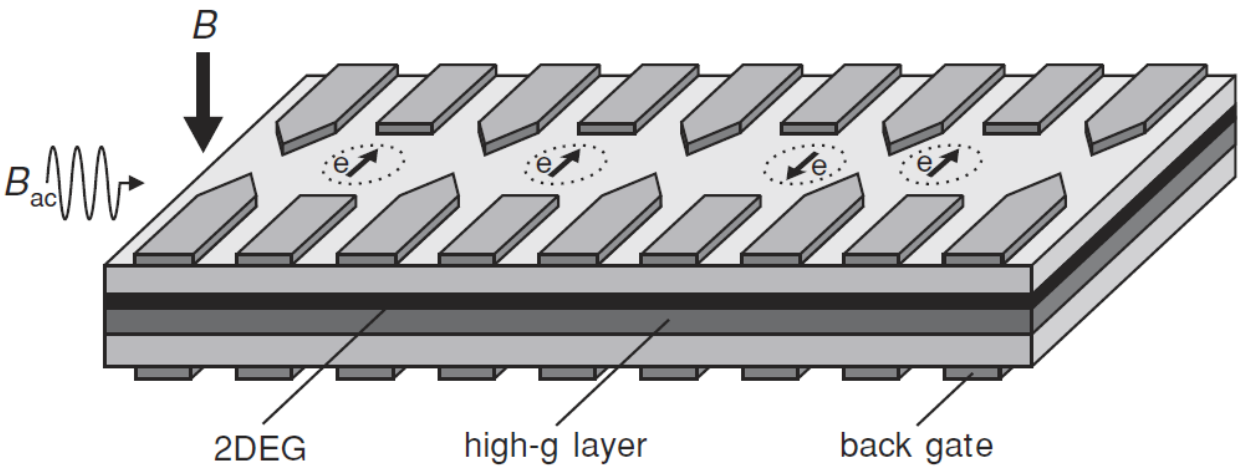

Fig. 2. Schematic picture of the spin qubit as proposed by Loss and DiVincenzo [2]. The array of metal electrodes on top of a semiconductor heterostructure, containing a two-dimensional electron gas (2DEG) below the surface, defines a number of quantum dots (*dotted circles*), each holding a single electron spin (*arrow*). A magnetic field, B, induces a Zeeman splitting between the spin-up and spin-down states of each electron spin. The spin state is controlled either via an oscillating magnetic field, B_{ac} (on resonance with the Zeeman splitting), or via an oscillating electric field created with the back gates, which can pull the electron wavefunction into a layer with a large g-factor. Coupling between two spins is controlled by changing the voltage on the electrodes between the two dots (Adapted from [2])

What is photovoltaics ?

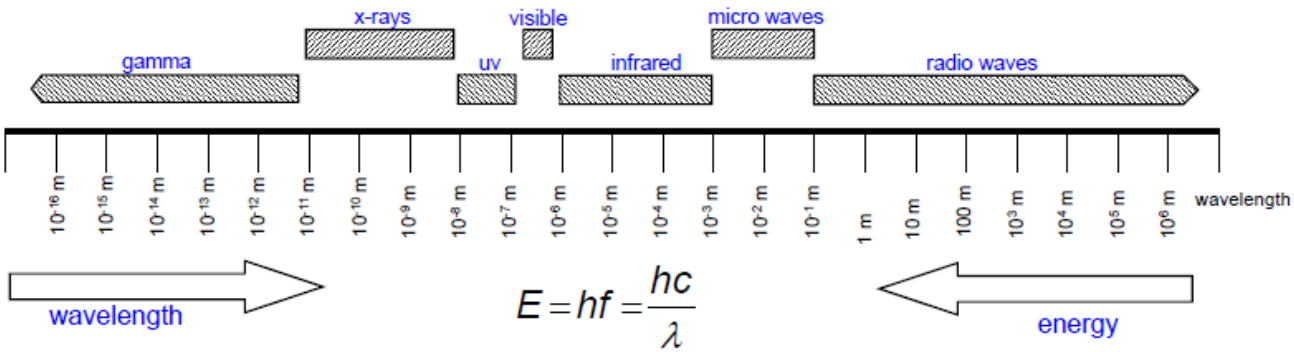

$$E = hf = \frac{hc}{\lambda}$$

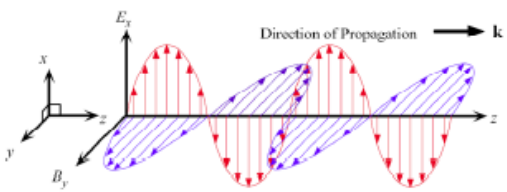

Photon propagation as an electromagnetic wave

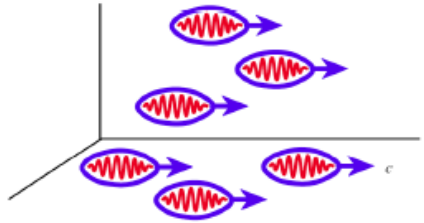

Representation of Light as a stream of Photons

Alexandre-Edmond BECQUEREL
(1820 – 1891)

The electrical effects in materials caused by interaction with Light was reported by Edmond Becquere (France) in 1839

Example of photovoltaic systems

Photovoltaic cell: working principle

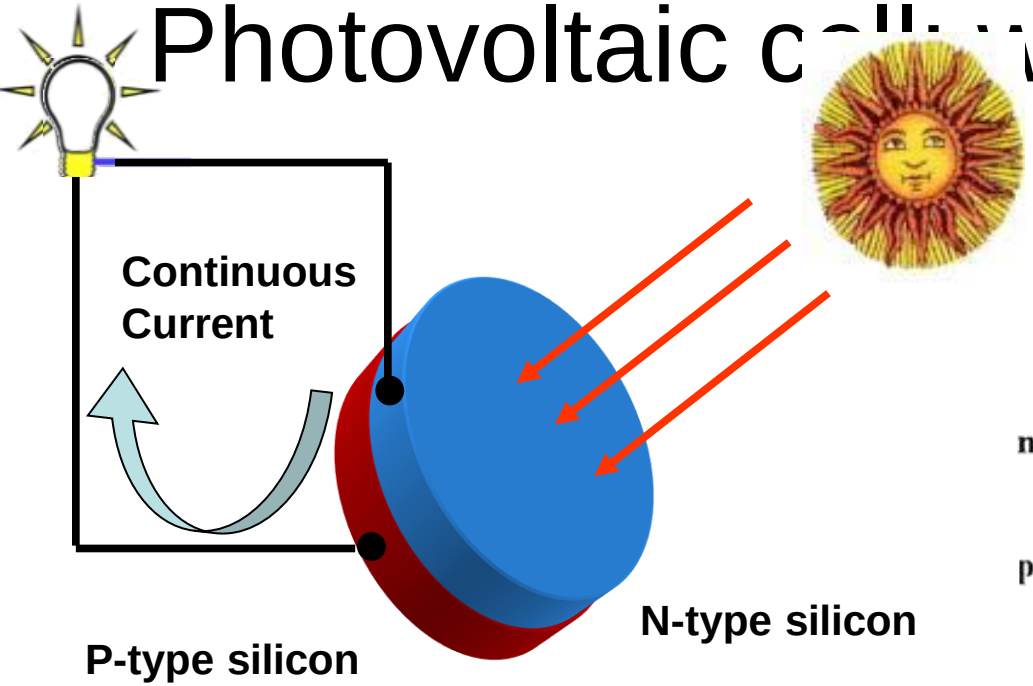

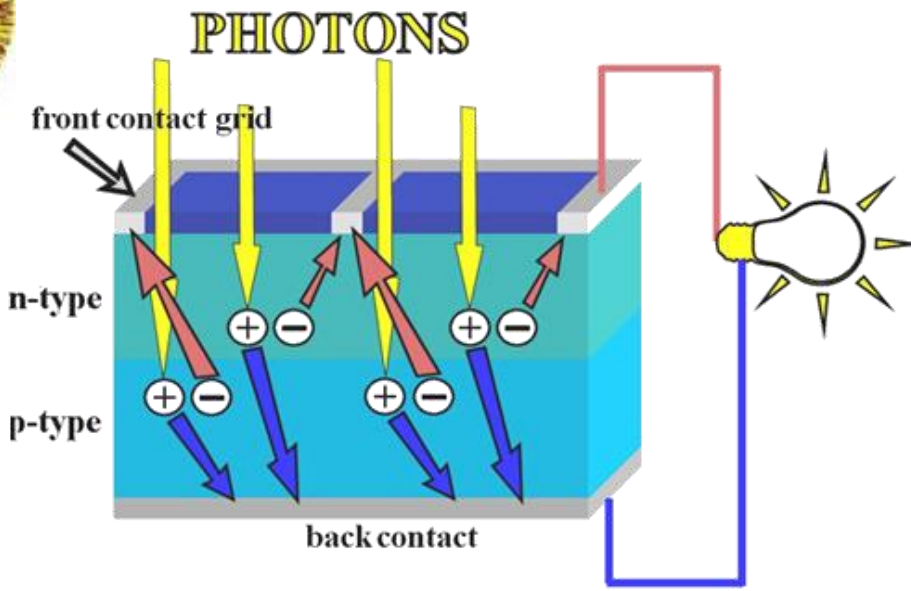

“Conventional” photovoltaic cells are based p-n junction between semiconductors. When charged by the sun, the cell generates a dc photovoltage of 0.5 to 1 volt.

Optical effects:

This can occur provided $\omega_{photon} > \omega_{gap}$

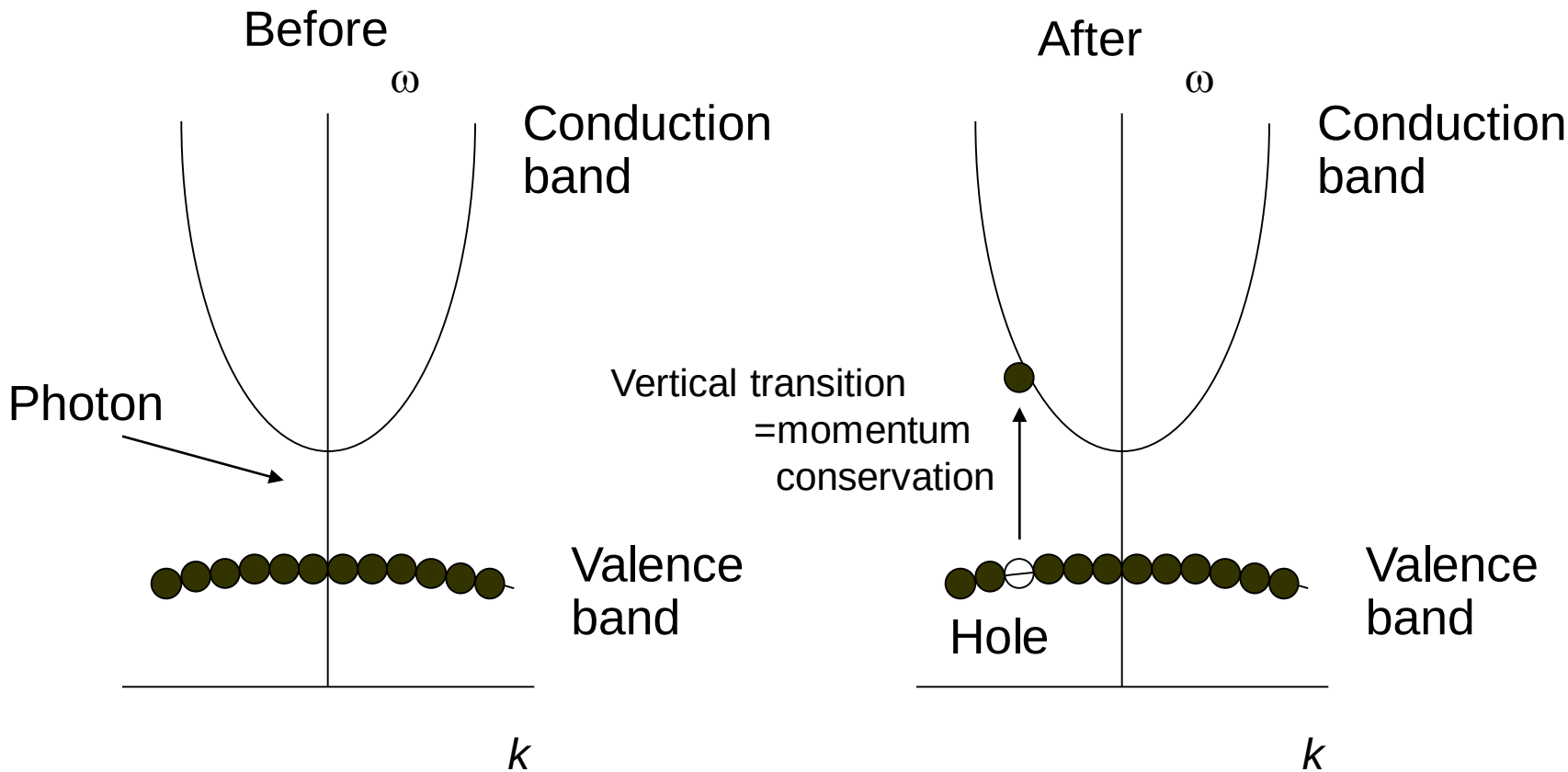

Optical properties :

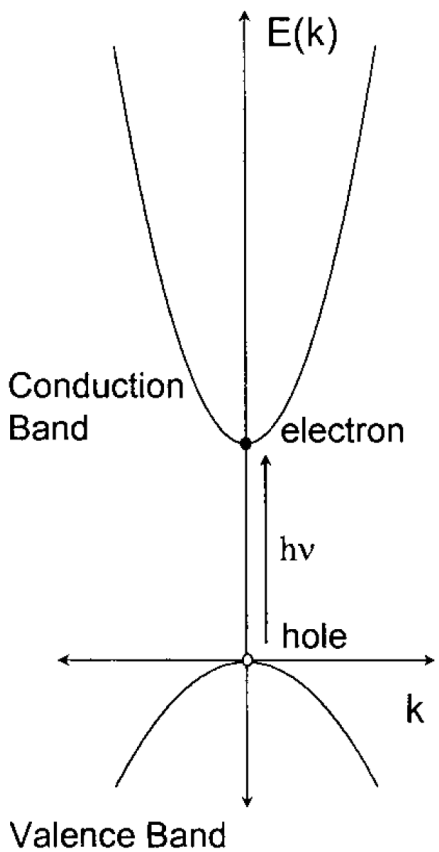

$$\psi_{\vec{K}}(\vec{r}) = \exp(i\vec{K}\vec{r})u_{\vec{K}}(\vec{r})$$

$$\varepsilon(\mathbf{K}) = E_c + \frac{\hbar^2 K^2}{2m_e^*}$$

$$\varepsilon(\mathbf{K}) = E_\nu - \frac{\hbar^2 K^2}{2m_h^*}$$

$$E_f = E_i + \hbar c Q, \quad \mathbf{K_f} = \mathbf{K_i} + \mathbf{Q}$$

direct indirect

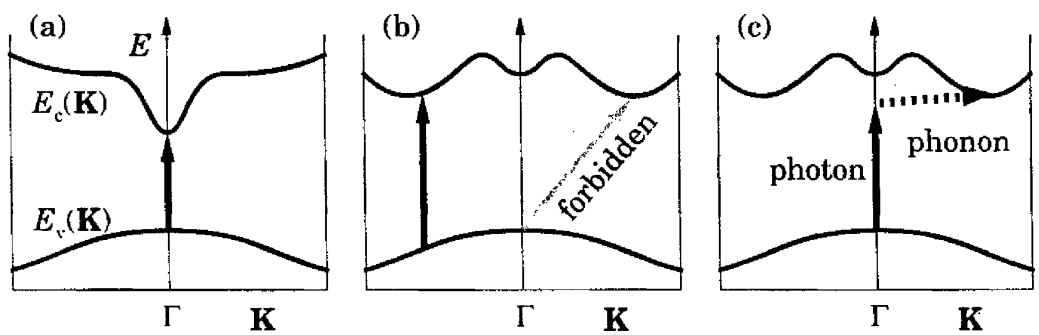

Efficiency

One of the most important parameters of the photovoltaic cell is the efficiency defined as:

$$\text{EFFICIENCY} = \eta = \frac{\text{Max electrical power produced by the cell}}{\text{Total solar power impinging on the cell}}$$

Example:

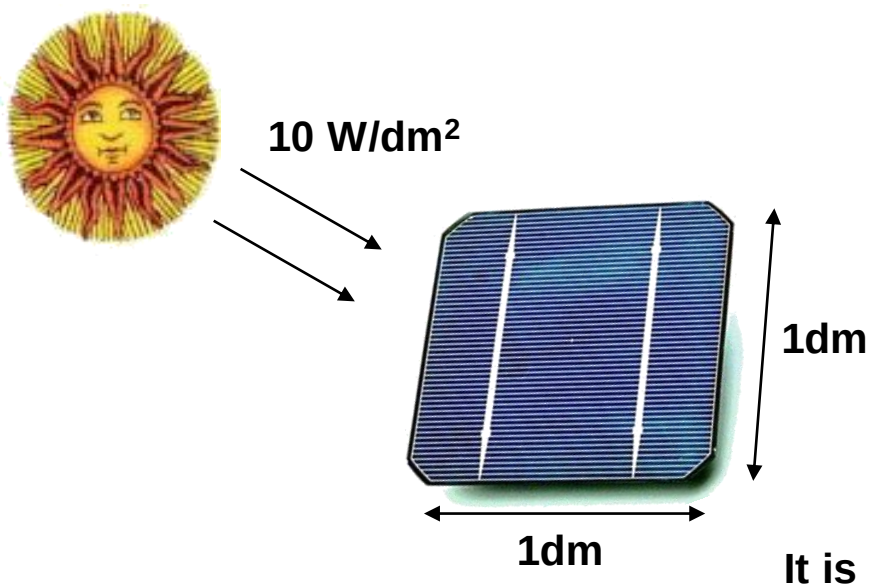

$\eta = 10\%$ → **1 W**

$\eta = 20\%$ → **2 W**

It is important to increase as much as possbile the efficiency.

Too keep things straight…

- ”Normal” crystalline Si homojunction solar cells are NOT bad solar cells!

  - Best crystalline Si solar cell efficiency: 24.7 % (1 Sun)
  - Best large area Si-based solar cell: 23.4 % (1 Sun)
  - Best large area Si-based solar module: ~ 20 %
  - Current market share: > 90 %
  - Energy payback times (solar energy system): ~ 2 years
  - Non-toxic and abundant raw materials
  - …




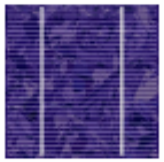


Solar spectrum

The amount of energy that reaches the earth's surface every year exceeds the total energy consumption by roughly a factor of 10000.

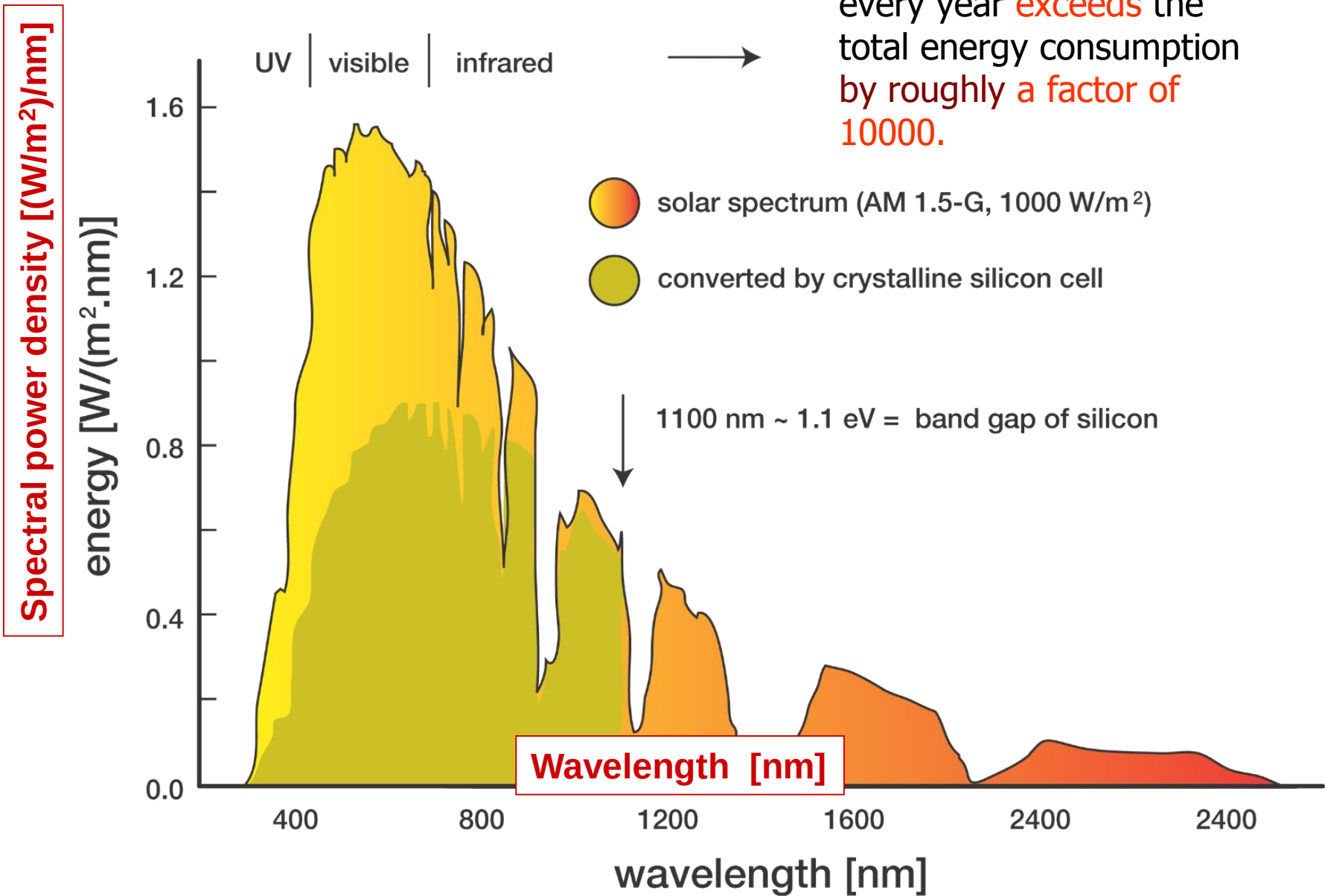

Semiconductor nanocrystals

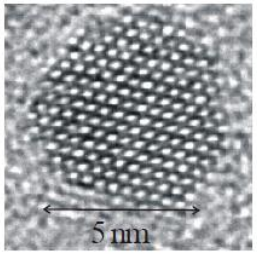

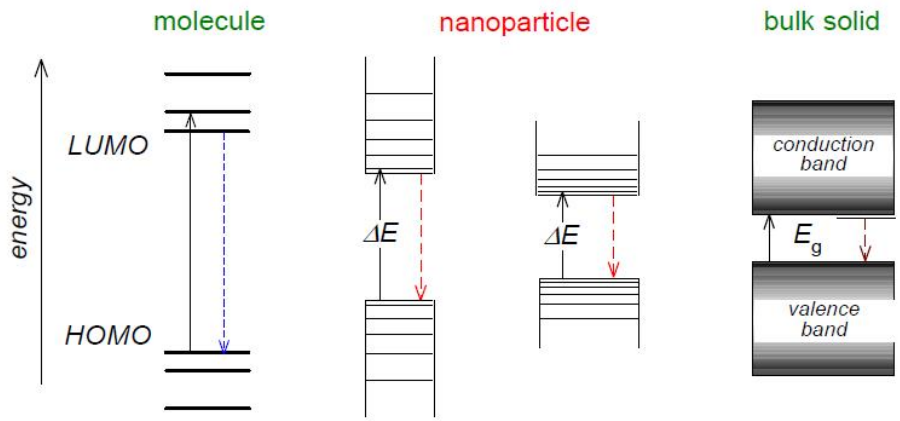

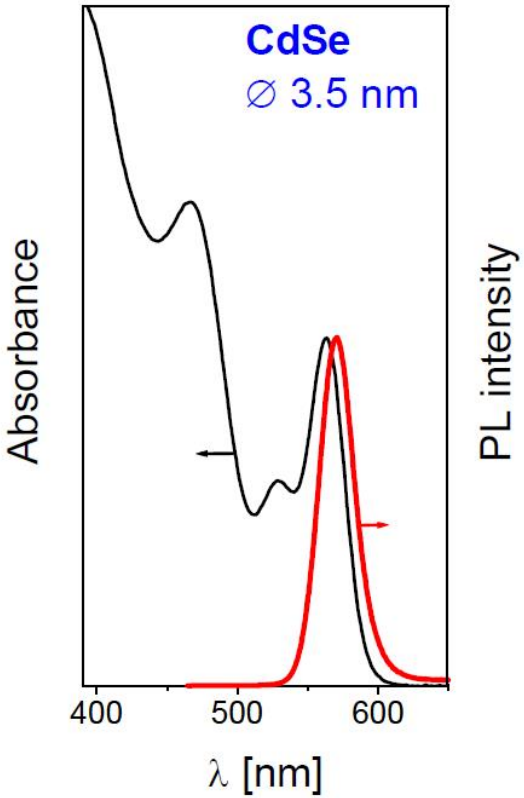

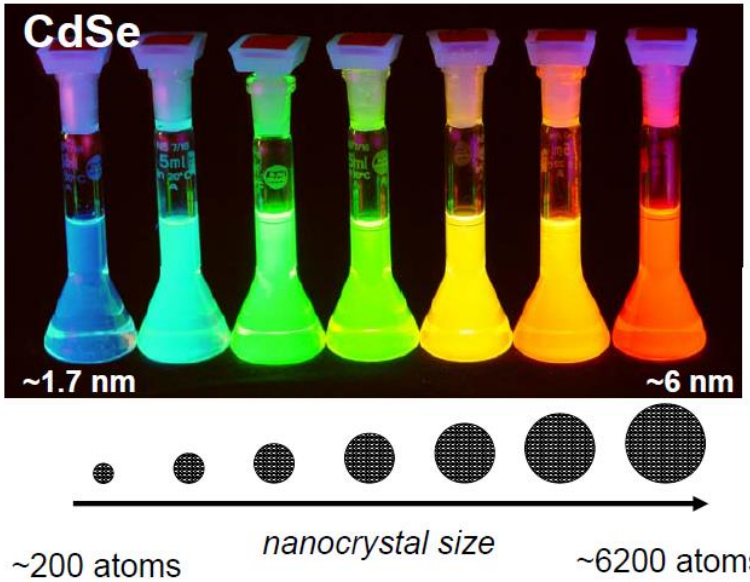

The pioneers

A. Ekimov
A. Efros
L. Brus

Ekimov, A.I. et al., "Quantum size effect in three-dimensional microscopic semiconductor crystals," *JETP Lett*, vol. 34, No. 6, Sep. 20, 1981, pp. 345-349.

Al. L. Efros, A. L. Efros. "Interband absorption of light in a semiconductor sphere." *Sov. Phys. Semicond*. 16, 1982, 772-775.

Ekimov, A.I. et al., "Quantum size effect in the optical spectra of semiconductor microcrystals," *Sov. Phys. Semicond*. 16(7), Jul. 1982, pp. 775-778.

Electronic Wave Functions in Semiconductor Clusters: Experiment and Theory

Louis Brus

AT&T Bell Laboratories, Murray Hill, New Jersey 07974 *(Received: December 26, 1985)*

J. Phys. Chem. **1986**, *90*, 2555–2560

$$E^* \simeq E_g + \frac{\hbar^2\pi^2}{2R^2}\left[\frac{1}{m_e} + \frac{1}{m_h}\right] - \frac{1.8e^2}{\epsilon R} + \text{smaller terms}$$

Properties of Quantum Dots:

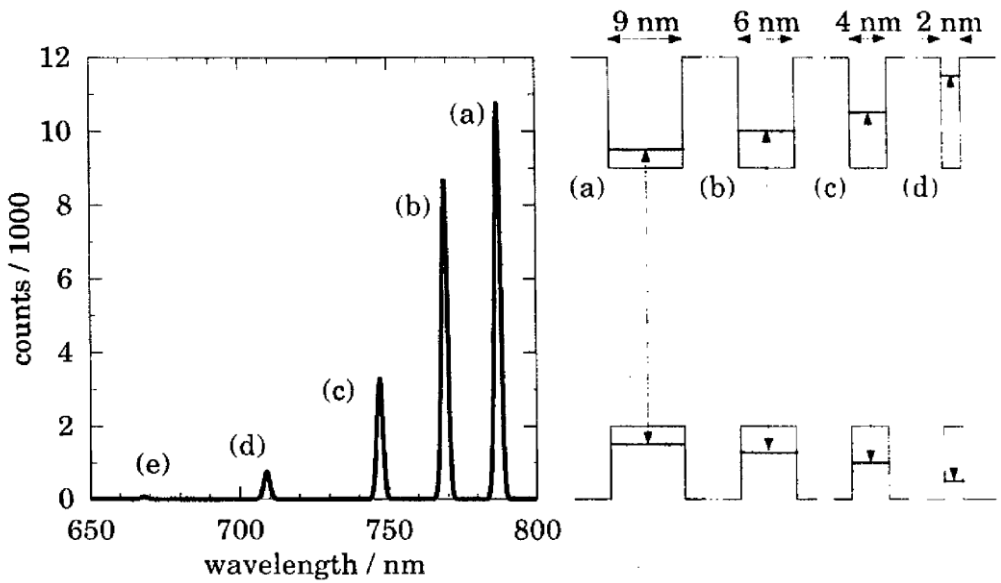

Control of the band gap energy (depends on the QD size). A mixture of different QDs (with a different size) allows to collect a full solar spectrum.

$$\hbar\omega = \varepsilon_{en} - \varepsilon_{hn} = (E_c + \frac{\hbar^2\pi^2n^2}{2m_e^*a^2}) - (E_\nu - \frac{\hbar^2\pi^2n^2}{2m_h^*a^2})$$

$$= E_g + \frac{\hbar^2\pi^2n^2}{2a^2}(\frac{1}{m_e^*} + \frac{1}{m_h^*})$$

A mixture of different QDs

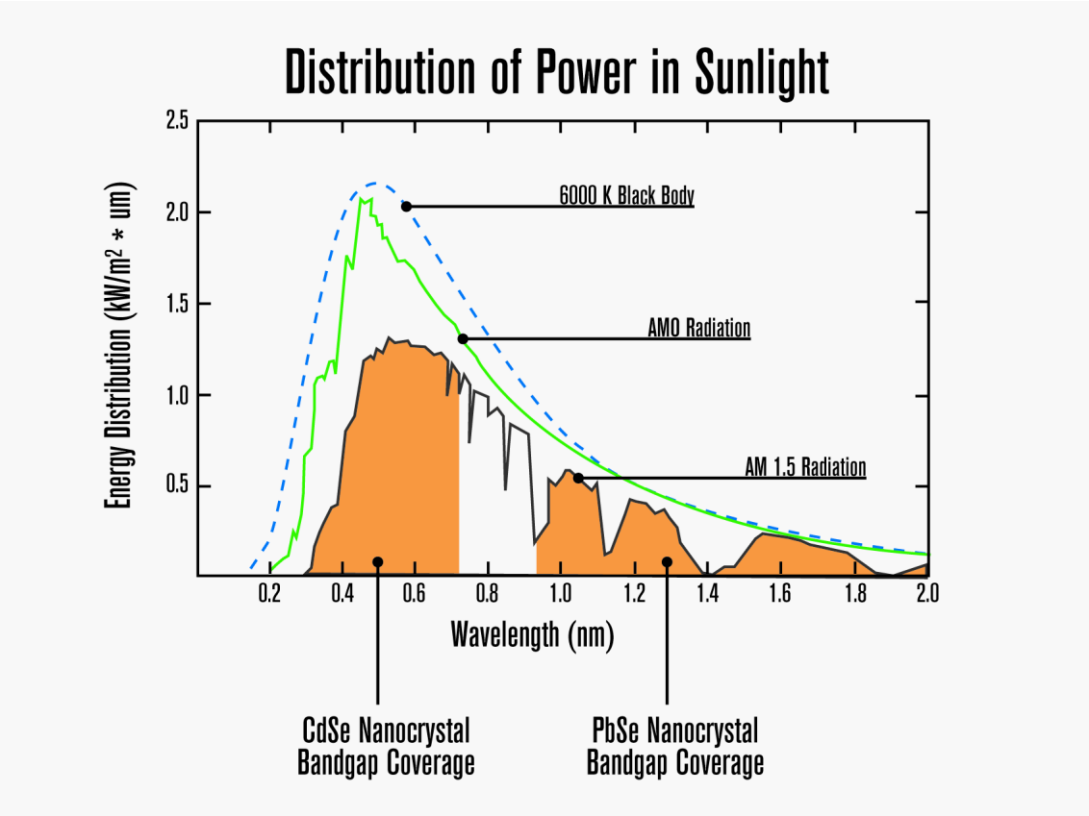

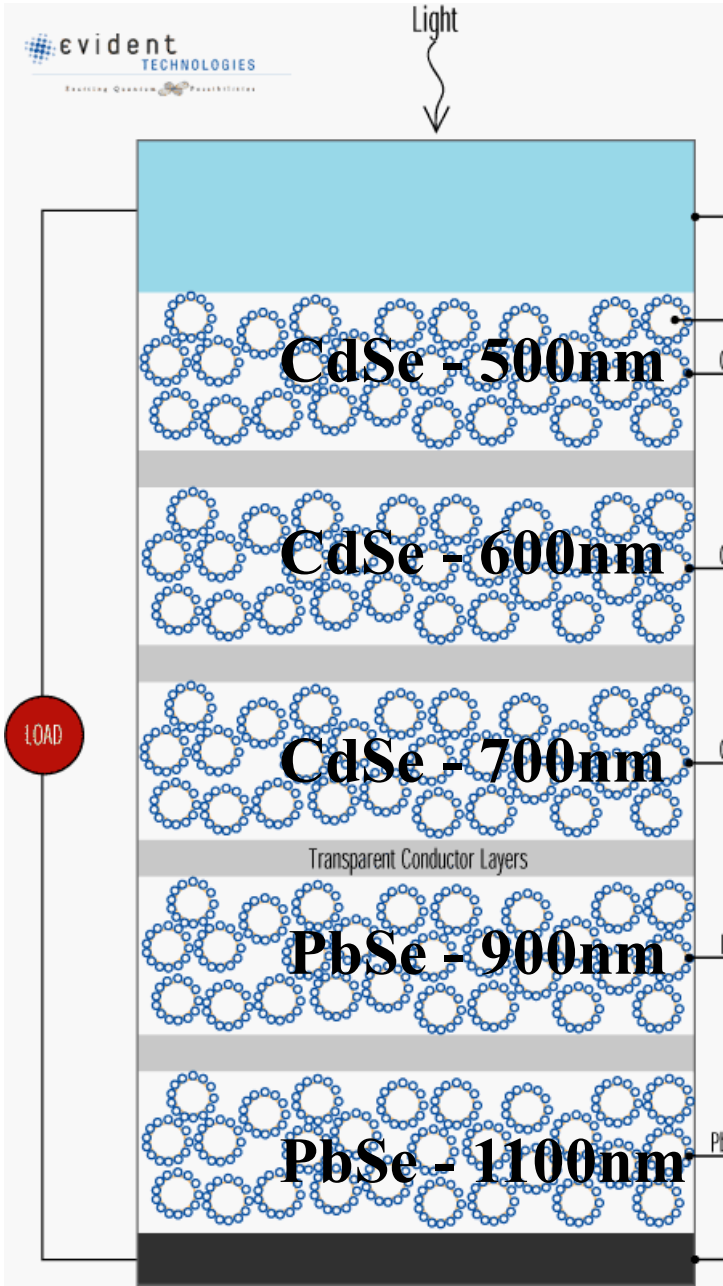

Optical properties :

$$\Delta E_e = \frac{h\nu - E_G}{1 + \frac{m_e^*}{m_h^*}}$$

Thermo-loss

$$\Delta E_h = (h\nu - E_G) - \Delta E_e$$

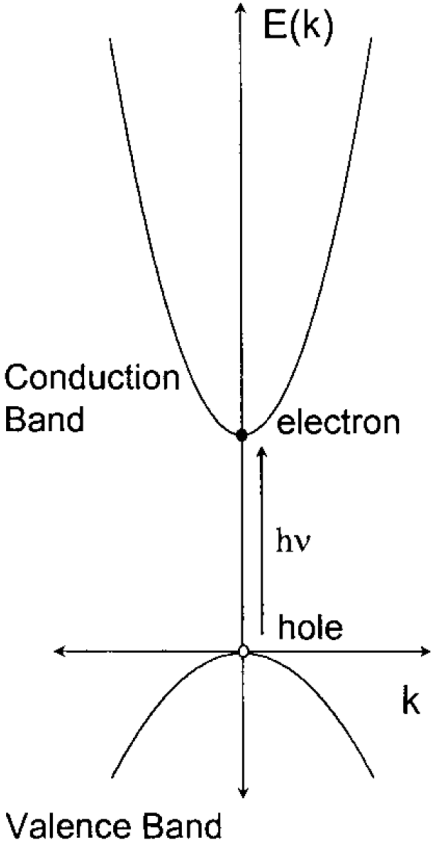

Conventional photovoltaic cell

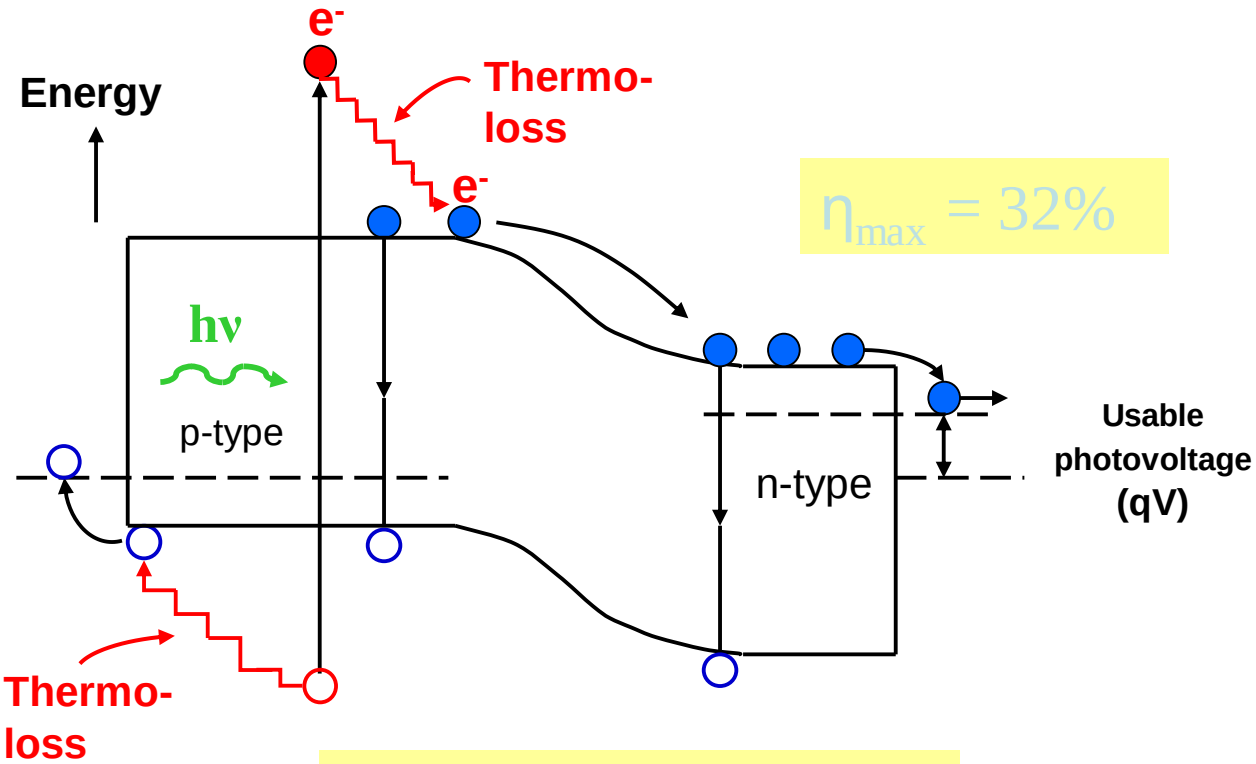

η_{max} = 32%

1 e^- - h^+ pair/photon

High Efficiency Multijunction Solar Cells

- Want 1eV material lattice-matched to GaAs

  ⇒ Try GaInNAs

Calculated efficiencies (ideal)

500X AM1.5D:	36%	47%	52%
One sun AMO:	31%	38%	41%

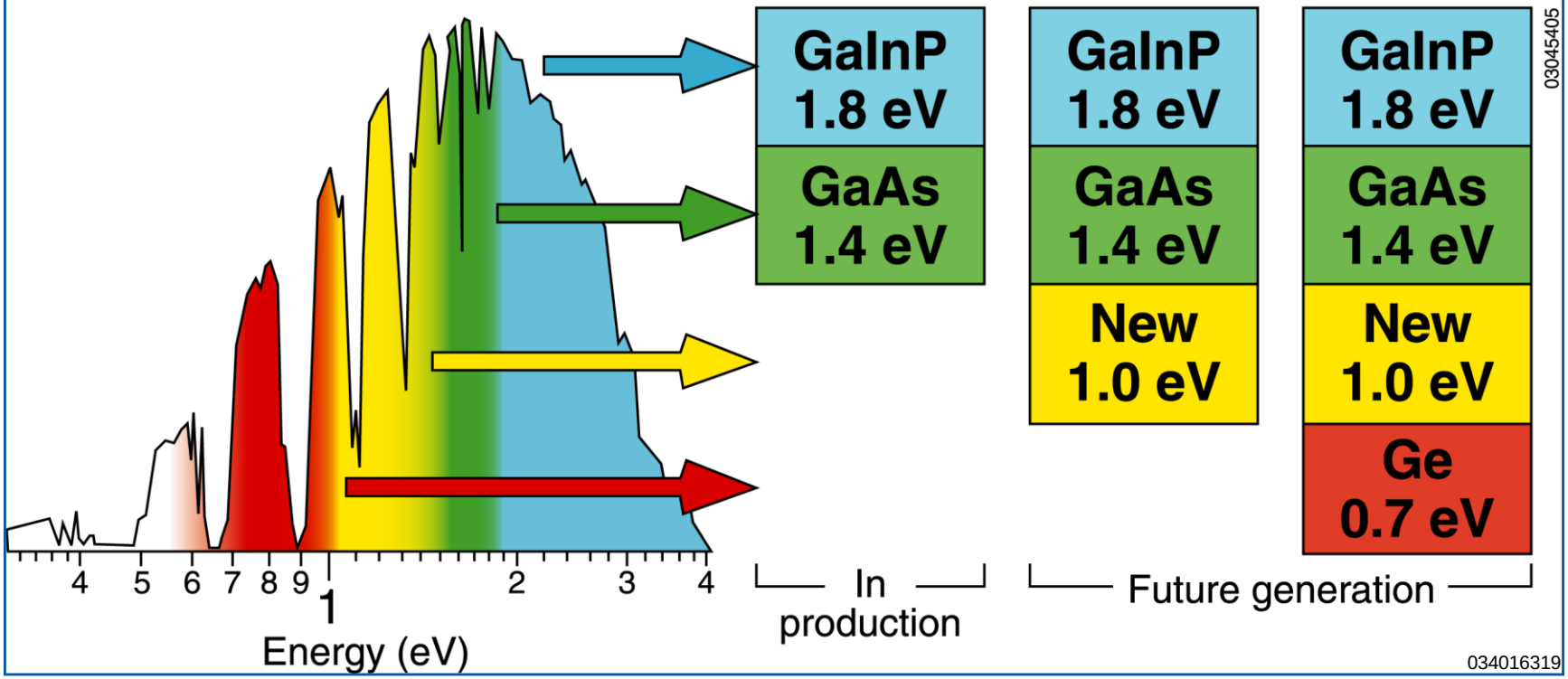

Multi-Exciton Generation (MEG)

Multiple-Exciton Generation by ONE absorbed photon

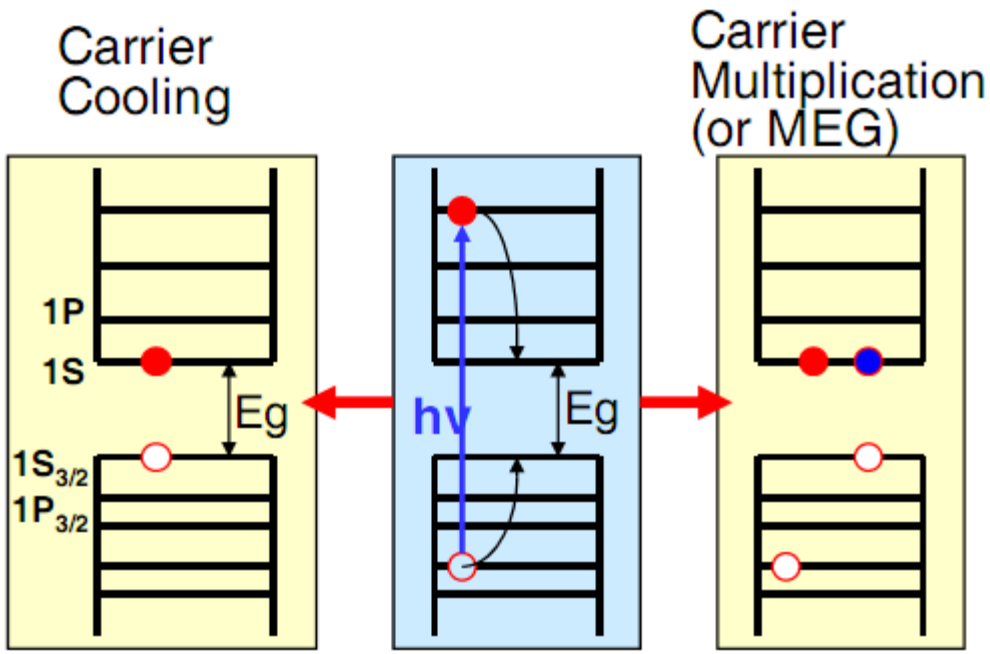

Effect of quantum confinement on:
Carrier relaxation
Exciton interaction (Annihilation and MEG)

MEG has been reported in:
CdSe, PbSe, PbS, PbTe, InAs, Si

Klimov
2004, PbSe: 2 excitons (PRL, 92, 186601)
2006: PbSe: 7 excitons (NanoLett, 6, 424)
2006: CdSe: (JPC B 110, 25332)
Nozik:
2005: PbSe, PbS (Nano Lett, 5, 865)
2006: PbTe (JACS, 128, 3241)
2007: PbSe film (Nano Lett, 7, 1779)
2007: Si (Nano Lett, 2007)
Bonn, Banin, Ruhman
2007: InAs (JPC C, 111,4146)
Prasad: (2008) (APL, 92, 031107)
PbSe photoconductor

MEG has been disputed:
Bawendi et al., PRB, 76, 081304R (2007)
Bonn, Banin, Ruhman, NL, (2008),8,1207

Coherent Superposition of Multi-Excitonic States in PbSe QDs

NanoLetts **5**, 865 (2005)

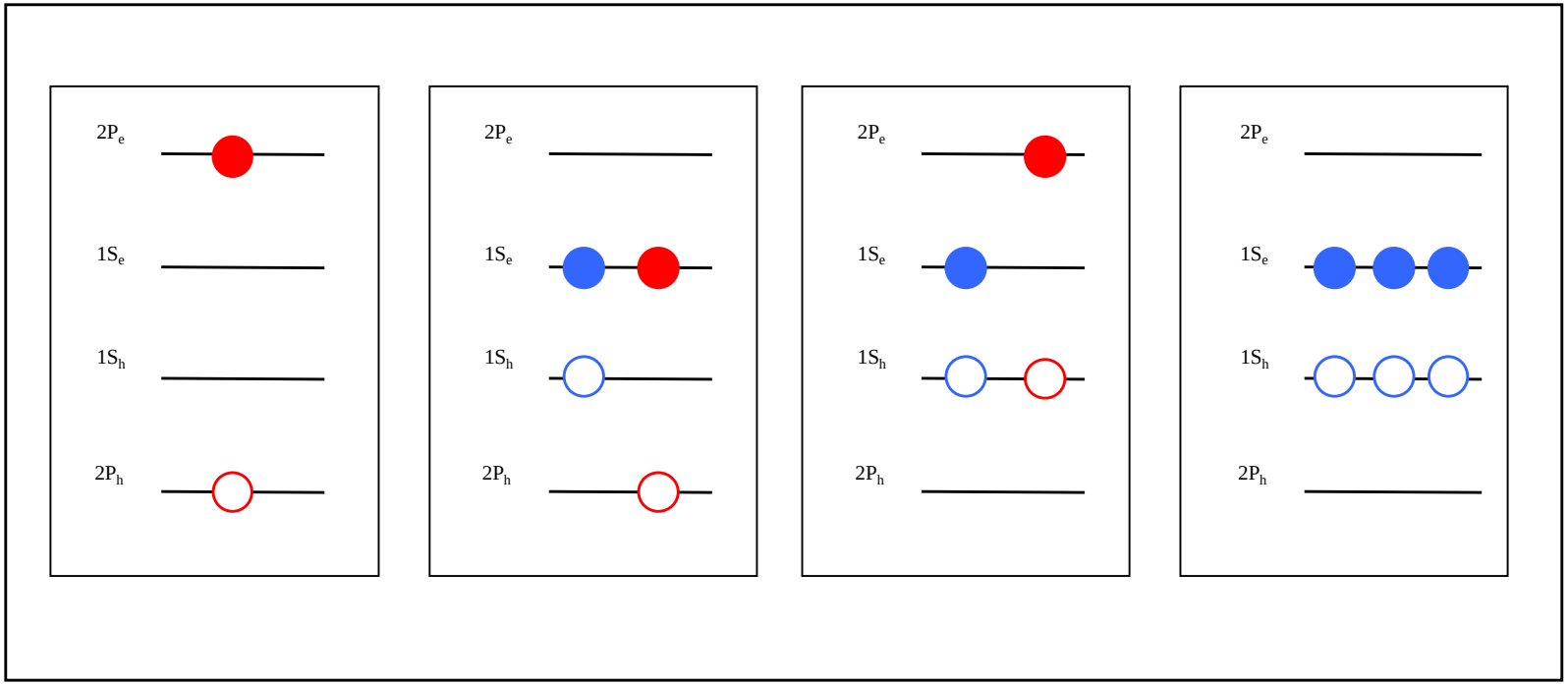

For QDs PbSe (diameter 2.9 nm) there were observed 3 excitons at photon energy which is about 4 E_{gap}

QDs technology basics

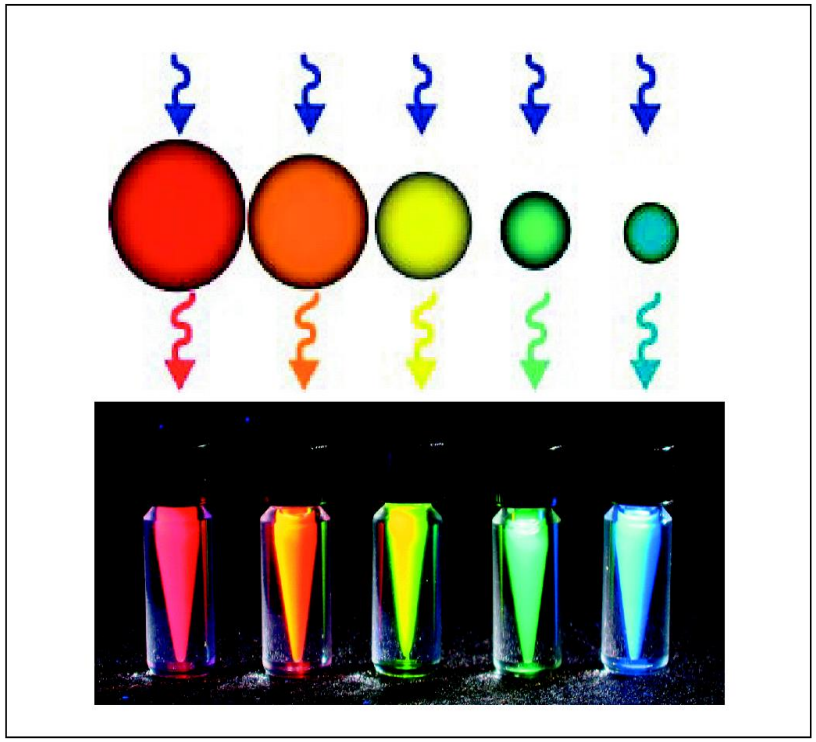

Figure 5. Different size quantum dots emit different color light. Quantum dots change emission color with size because additional energy is required to "confine" the semiconductor excitation to a smaller volume. Any light source "bluer" than the dot of interest can be used.

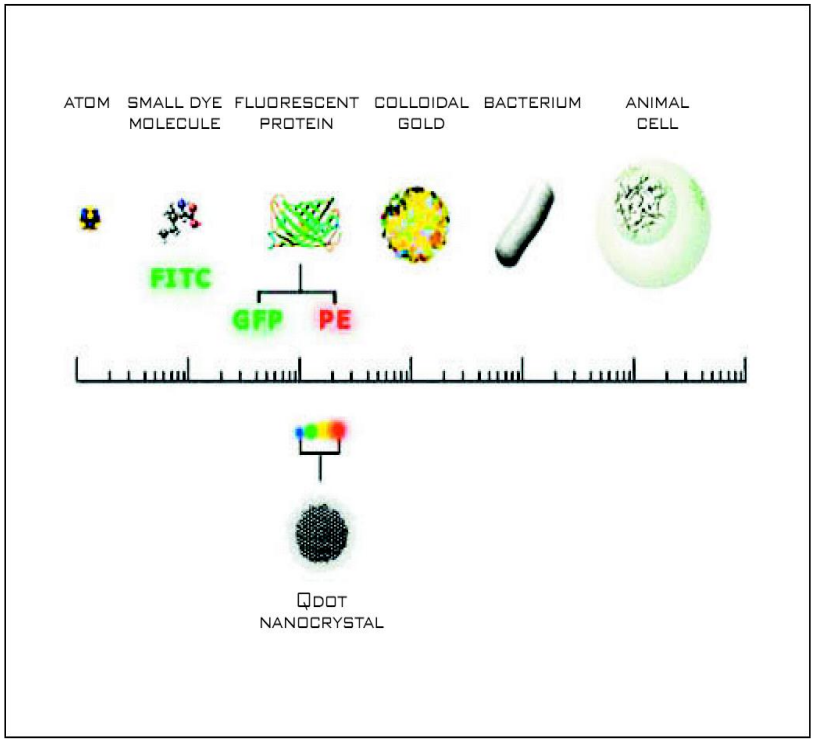

Figure 6. Relative size of a quantum dot. Quantum dots are about the size of a large macromolecule or protein. Qdot Streptavidin Conjugates range in size from 10–15 nanometers in diameter.

Two Flavors of Quantum Dots: *Epitaxial and Nanocrystal Quantum Dots*

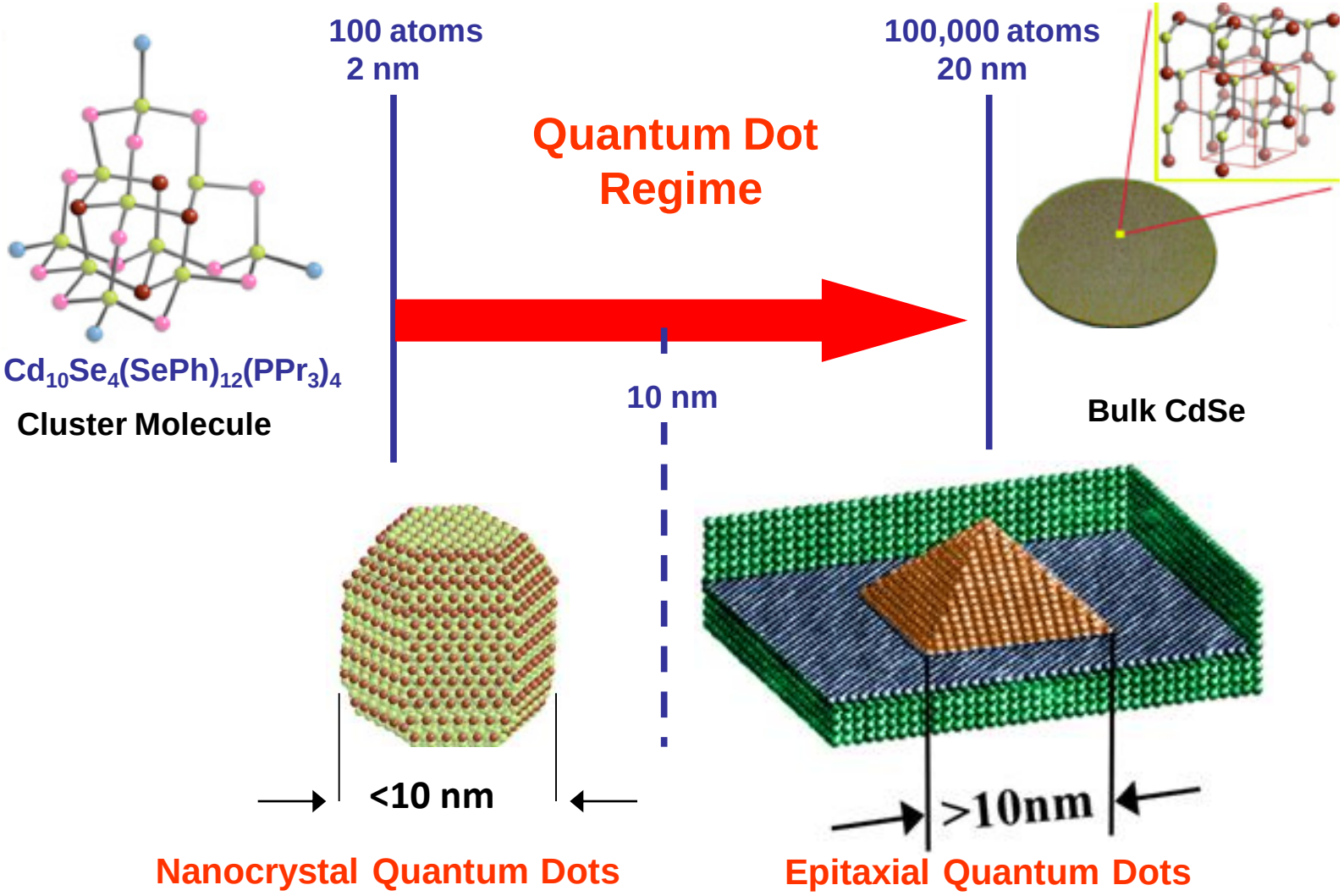

Core-Shells and other Nano-heterostructures

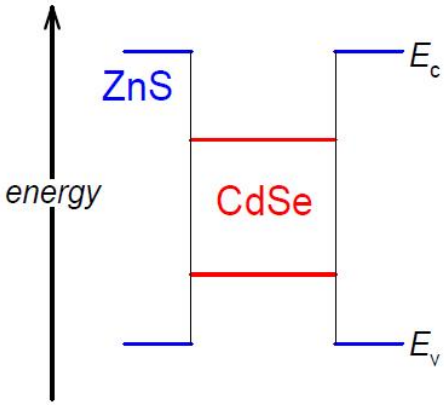

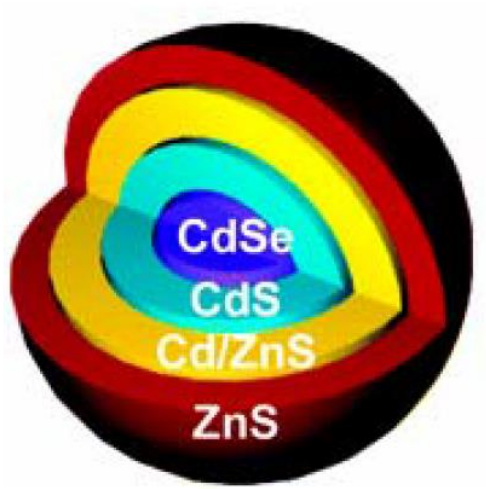

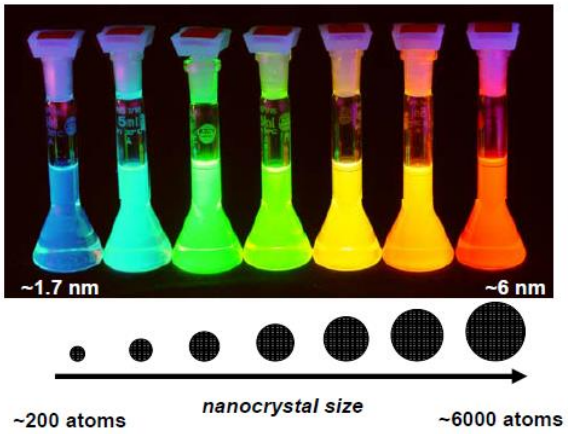

Band gap and strain engineering in core-shell nanocrystals

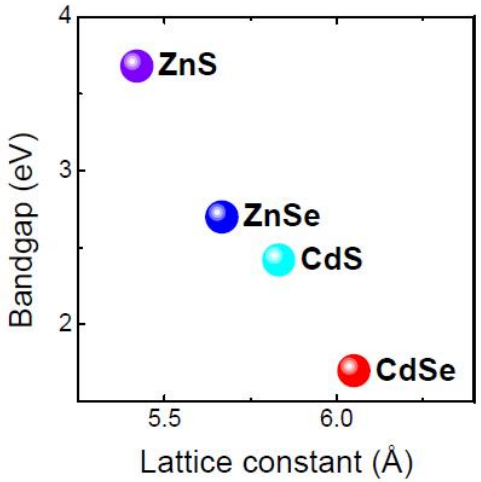

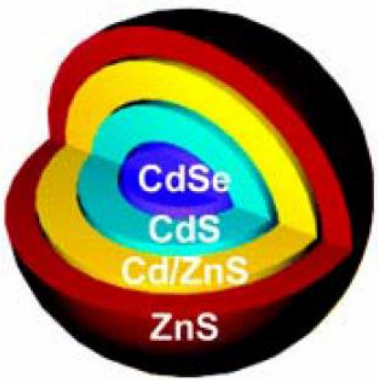

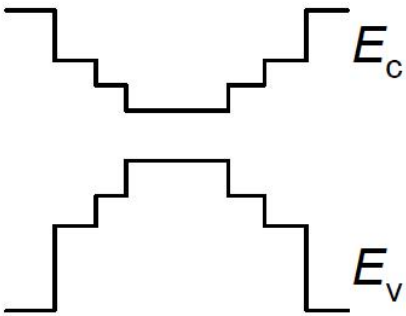

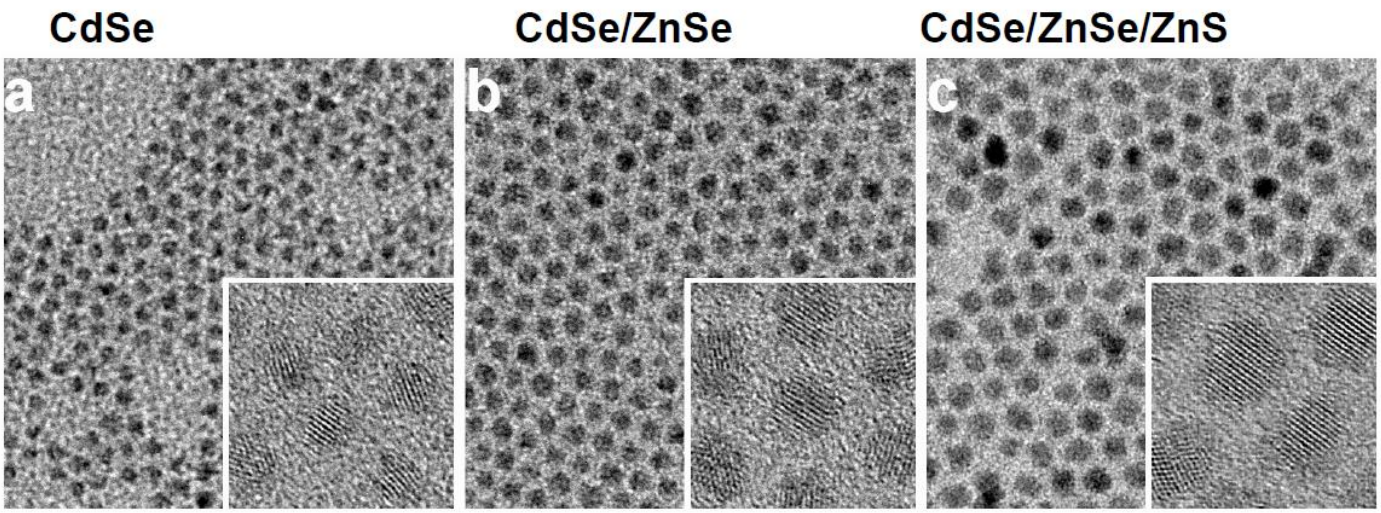

J. Phys. Chem. B 2004, 108, 18826.

Editors' Choice: Science 2004, vol. 306, p. 1439.

QDs technology basics (biology)

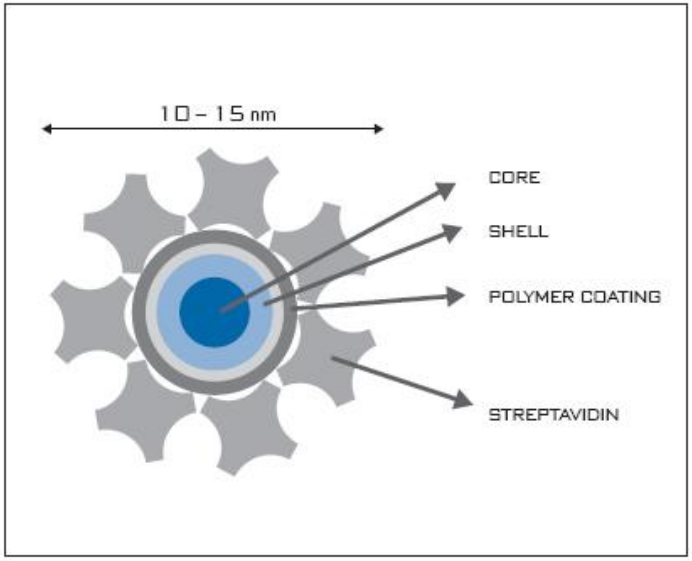

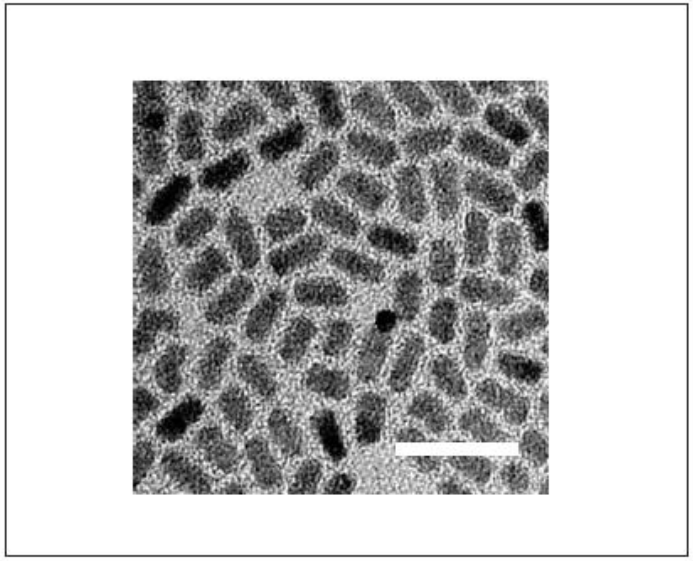

What is a Qdot Conjugate?

The new high-performance class of Qdot Conjugate fluorescent labeling reagents leverages the unique properties of state-of-theart quantum dot technology. Quantum dots are nanometer-scale semiconductor crystals (Figure 2) with special optical properties. Each Qdot Conjugate has a quantum dot core composed of semiconductor material (CdSe), which has been coated with an additional semiconductor shell (ZnS) to improve its optical properties. This inner core is then further coated with a polymer shell that can be conjugated to biomolecules while retaining the optical properties of the Qdot nanocrystal (Figure 1). For the Qdot Streptavidin Conjugates, these polymer-coated quantum dots have been directly coupled to streptavidin.

scale=20nm
Amplification 200 000X

QDs replace organic dyes !

QDs for biosensing

Dubna University develops the lateral immunochromatographic test-systems using quantum dots CdTeSe/CdS/CdZnS/ZnS, luminescent in the near-IR region of the spectrum

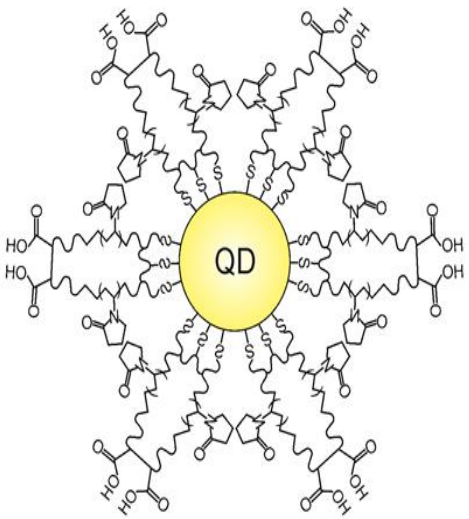

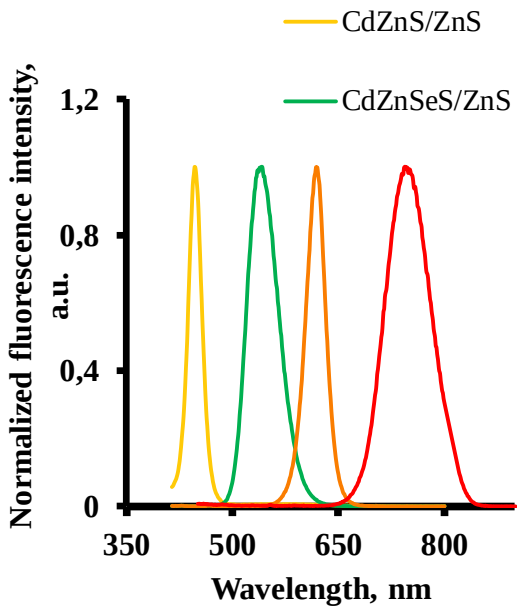

Advantages of QDs:

- A wide absorption spectrum and a narrow peak of fluorescence
- High photostability
- A high quantum yield of fluorescence (50-70%)
- The presence of the necessary functional groups on the surface for further conjugation

1. Dezhurov, et al., **One-pot synthesis of polythiol ligand for highly bright and stable hydrophilic quantum dots toward bioconjugate formation** // Advances in Natural Sciences: Nanoscience and Nanotechnology, **9** (2018) 015002

Не удается отобразить рисунок.

From nanostructures to macroscopic materials

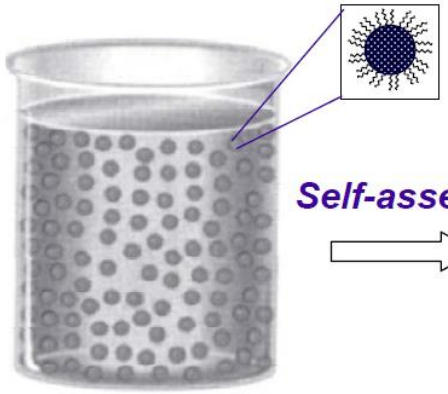

Self-assembly

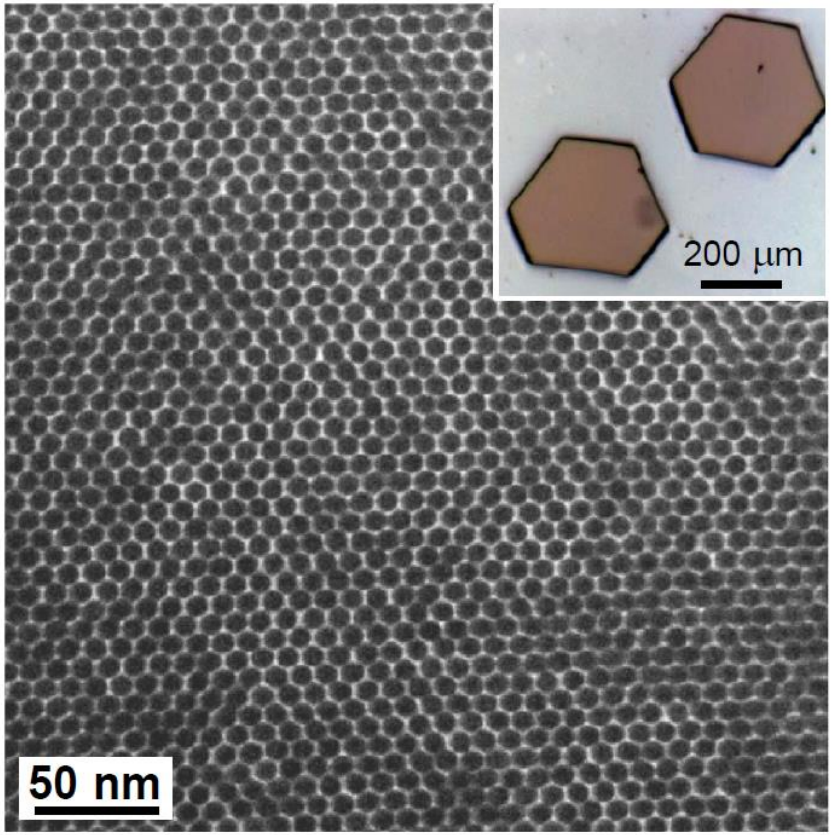

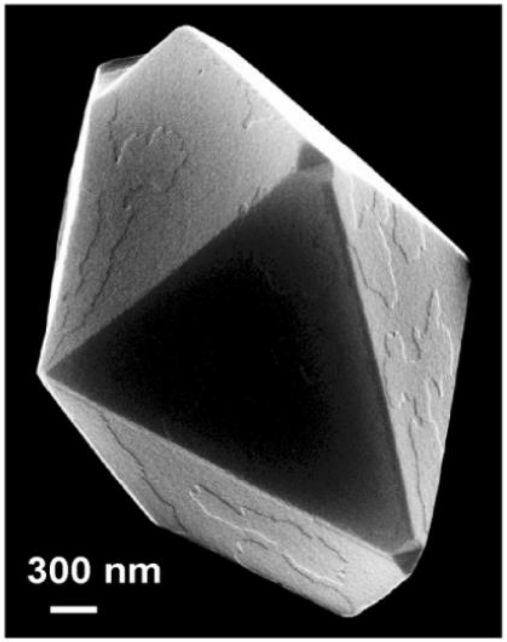

Rupich, Shevchenko, Bodnarchuk, Lee, Talapin. *J. Am. Chem. Soc.* **2010**, *132*, 289.

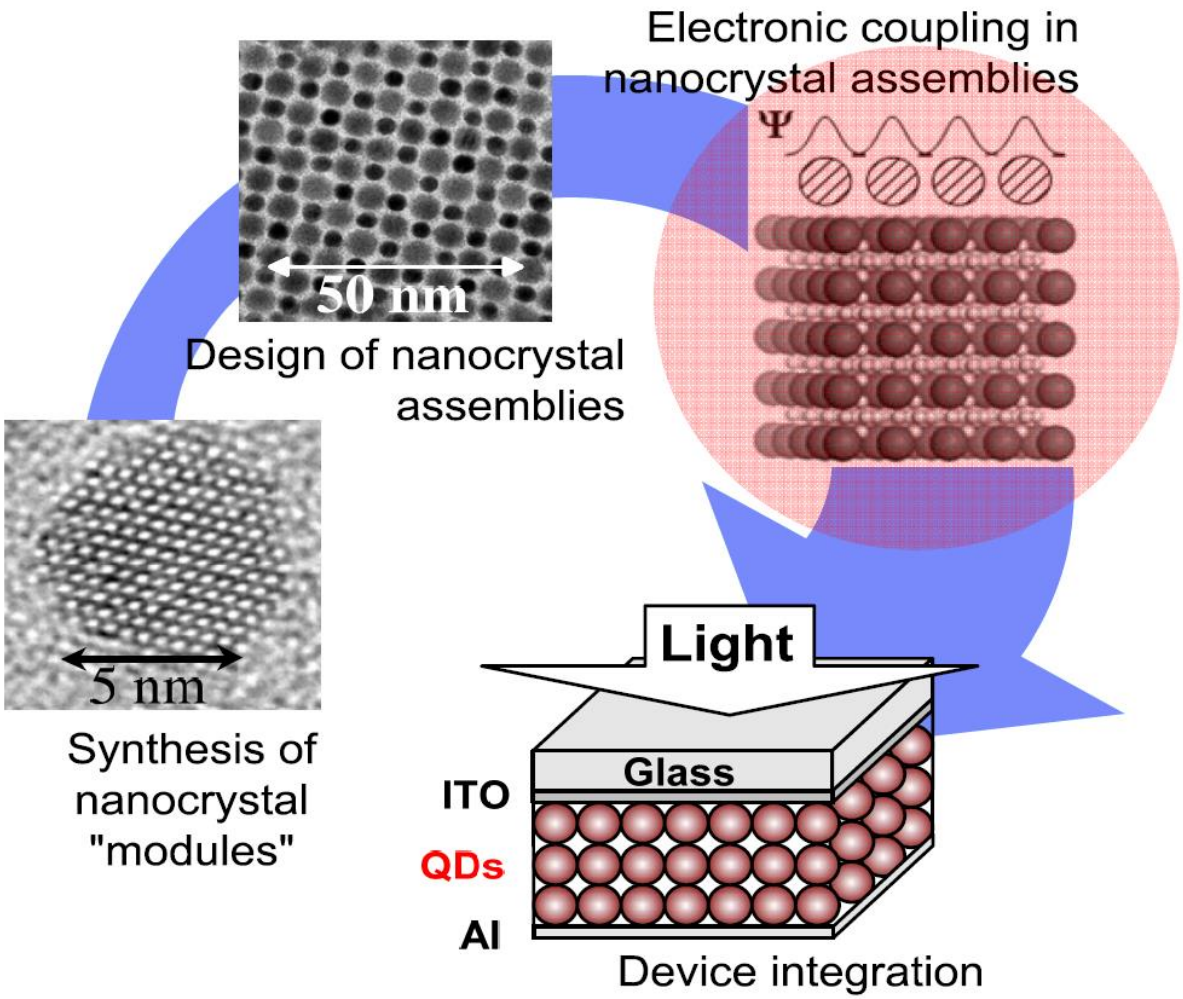
Electronic coupling in nanocrystal assemblies
Ψ
50 nm
Design of nanocrystal assemblies
5 nm
Synthesis of nanocrystal "modules"
Light
Glass
ITO
QDs
Al
Device integration

Usefulness of nanocrystal-based materials depends on their optical and electronic properties...

Single Crystals

Nanocrystalline Solids

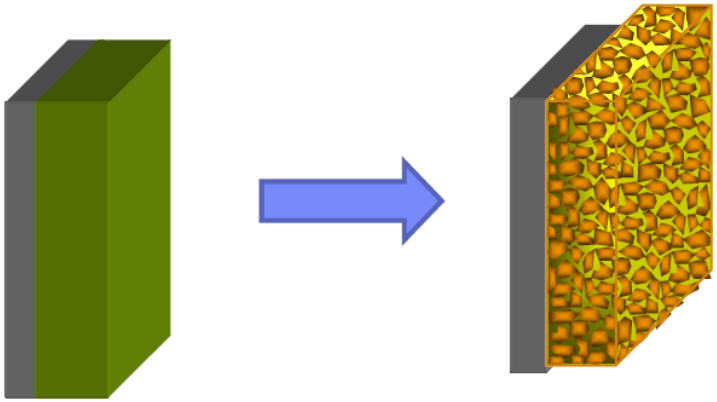

Good electronic properties of nanocrystal solids may open new doors to:

- photovoltaics
- thermoelectrics
- LED's
- photodetectors
- printable electronics

Quantum Cascade (QC) Laser

Operates within the sub-bands of the Conduction band. It is different from other designs where emission is due to electron-hole recombination. Often called Unipolar Laser. In conventional semiconductor lasers one electron can emit only one photon as it combines with a hole. QC laser is a Multiple Quantum Well (MQW). Discovered in 1996 (Appl. Phy. Lett. 68, 3680).

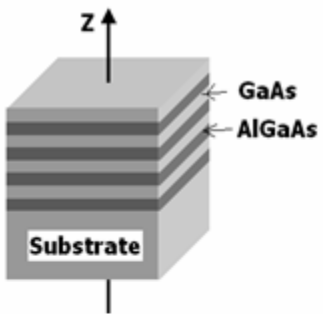

Multiple Quantum Well (GaAs/AlGaAs)

There could be ~50 Quantum Wells in MQW geometry. The barrier layer is very thin (1-3 nm) An excited electron emits 25-75 photons as it cascades down the ladder of sub-bands in the Conduction Band. QC lasers have been demonstrated for wavelengths between 3-20 micron. Useful for sensing atmospheric pollution

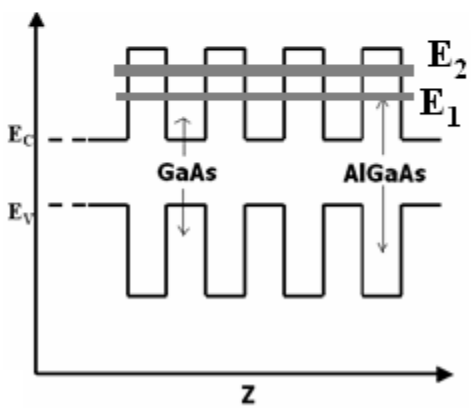

Energy Bands of MQW

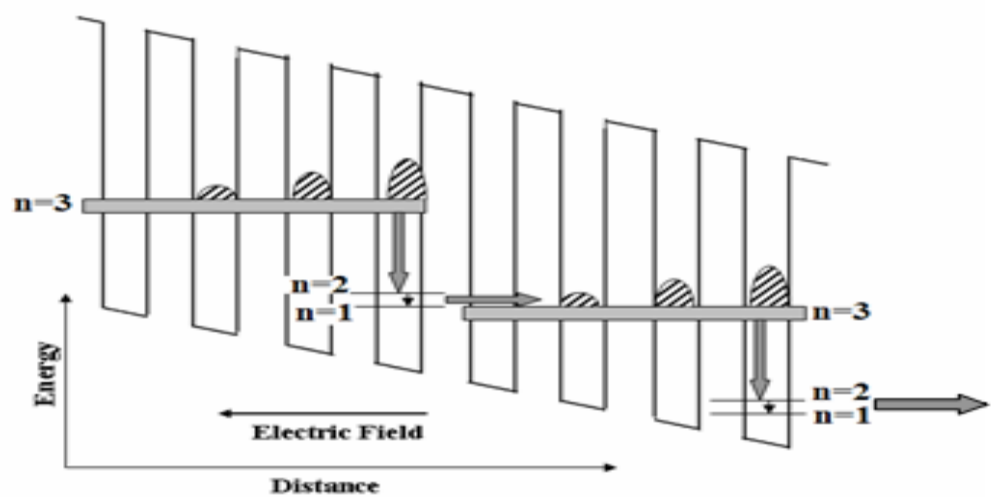

Energy Level Diagram in a QC Laser

The Lycurgus Cup (glass; British Museum; 4th century A. D.)

When illuminated from outside, it appears green. However, when Illuminated from within the cup, it glows red. Red color is due to very small amounts of gold powder (about 40 parts per million)

Dielectric materials:

All charges are attached to specific atoms or molecules

Response to an electric field *E*:

Microscopic displacement of charges

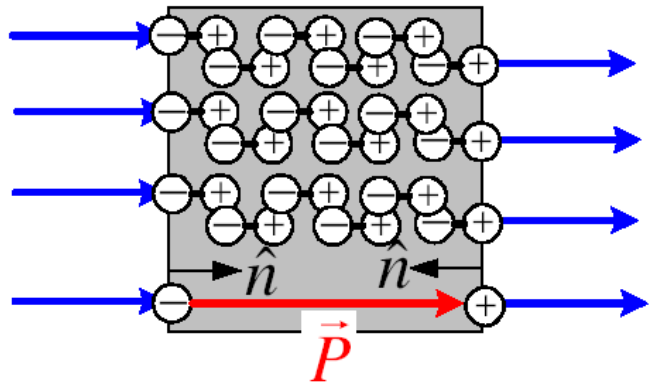

$$\vec{P} = \varepsilon_0 \chi \vec{E} = \varepsilon_0 (\varepsilon - 1) \vec{E}$$

Macroscopic material properties: electric susceptibility χ, dielectric constant (or relative dielectric permittivity) ε

What is a plasmon?

"plasma-oscillation": density fluctuation of free electrons

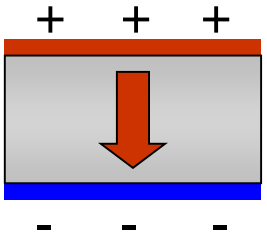

Plasmons in the bulk oscillate at $\omega_p^{drude} = \sqrt{\frac{Ne^2}{m\varepsilon_0}}$

determined by the free electron density and effective mass

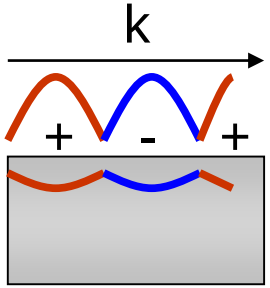

Plasmons confined to surfaces that can interact with light to form propagating "surface plasmon polaritons (SPP)"

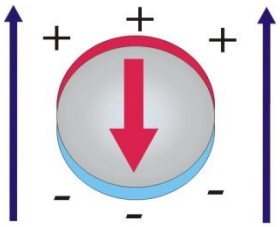

Confinement effects result in resonant SPP modes in nanoparticles

Sphere in a uniform static electric field

→ particle can be considered as a dipole:

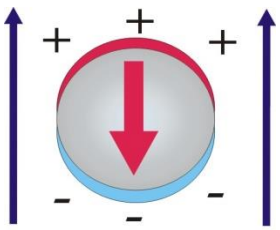

in a metal cluster placed in an electric field, the negative charges are displaced from the positive ones

$$\vec{p} = \boxed{4\pi\varepsilon_0 R^3 \frac{\varepsilon - \varepsilon_m}{\varepsilon + 2\varepsilon_m}} \varepsilon_m \vec{E}_0$$

electric polarizability of a sphere α

$$\alpha = 4\pi\varepsilon_0 R^3 \frac{\varepsilon - \varepsilon_m}{\boxed{\varepsilon + 2\varepsilon_m}}$$

$$\varepsilon = \varepsilon_1(\omega) + i\varepsilon_2(\omega)$$

dielectric constant of the metal particle

resonant enhancement of p

$$\boxed{\left|\varepsilon(\omega) + 2\varepsilon_m\right| = \text{minimum}}$$

ε_m = dielectric constant of the embedding medium, usually real.

→ If negative real dielectric constant $\varepsilon_1(\omega)$

Invisibility of plasmonic nanoshells

M. Kerker, J. Opt. Soc. Am. **65**, 376 (1975)

$$\beta = (a_c/a_s)^3$$

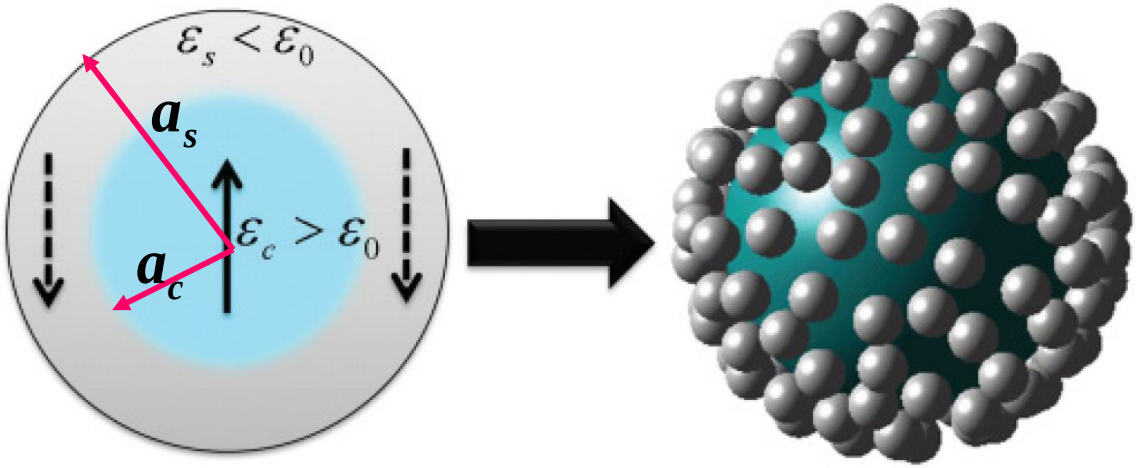

FIG. 1. (Color online) Schematic of the dielectric sphere to be cloaked surrounded by metallic nanoparticles (right) forming an effective invisibility shell (left) described by its effective permittivity ε_s and effective polarization vector (dashed arrows) $\mathbf{P}_s = \varepsilon_0(\varepsilon_s - 1)\mathbf{E}$ of opposite direction and same amplitude as the vector of the bare object (solid arrow) $\mathbf{P}_c = \varepsilon_0(\varepsilon_c - 1)\mathbf{E}$, where $\mathbf{E}$ is the local electric field and where our background material is air.

Narrow optical filtering with plasmonic nanoshells

Martynov, Nazmitdinov,Tanachev, Gladyshev, JETP Letters **95** (2012)122

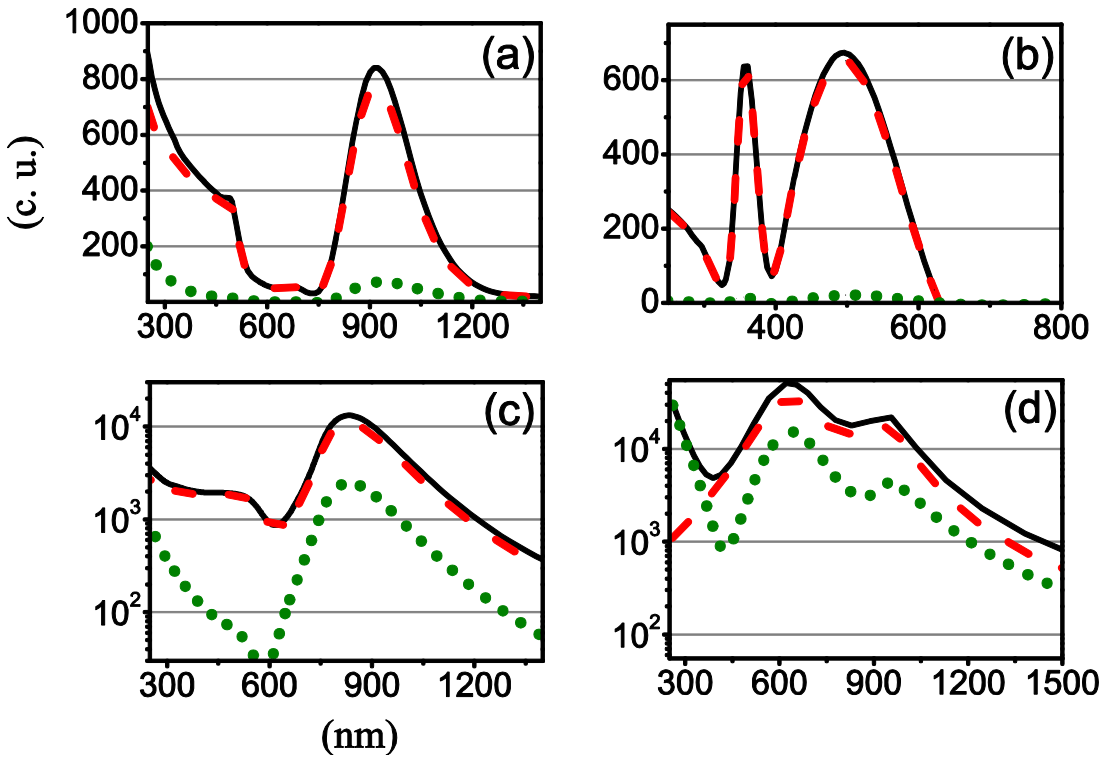

$$\sigma_{ext} = \sigma_{sc} + \sigma_{abs}$$

$$\sigma_{sc} = \frac{8\pi}{3} \boldsymbol{k}^4 |\alpha|^2$$

$$\sigma_{abs} = 4\pi \boldsymbol{k} \ \mathrm{Im}(\alpha)$$

$$\boldsymbol{k} = \sqrt{\varepsilon_m}\,\omega / \boldsymbol{c}$$

$$\alpha = a_s^3 \frac{(\varepsilon_s - \varepsilon_m)(\varepsilon_c + 2\varepsilon_s) + \beta(\varepsilon_m + 2\varepsilon_s)(\varepsilon_c - \varepsilon_s)}{(\varepsilon_s + 2\varepsilon_m)(\varepsilon_c + 2\varepsilon_s) + 2\beta(\varepsilon_s - \varepsilon_m)(\varepsilon_c - \varepsilon_s)}$$

Field concentration in nanoshells d=40 nm

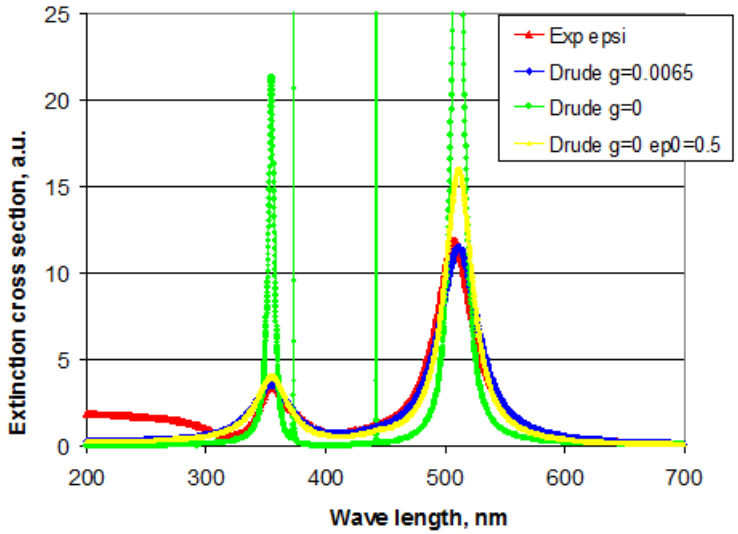

Dipole resonance near 500 nm

Quadrupole resonance near 450 nm

Dipole resonance near 500 nm with dissipation

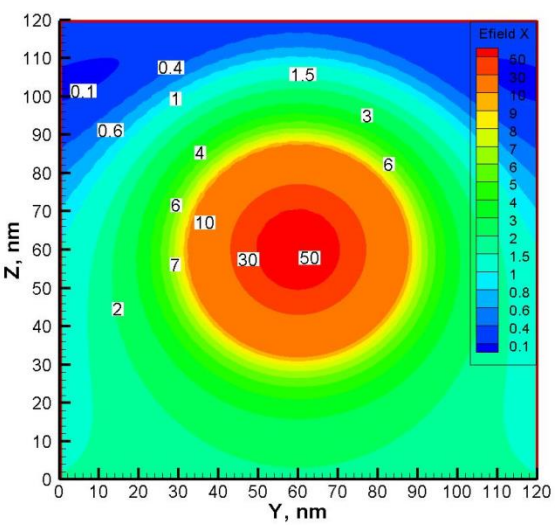

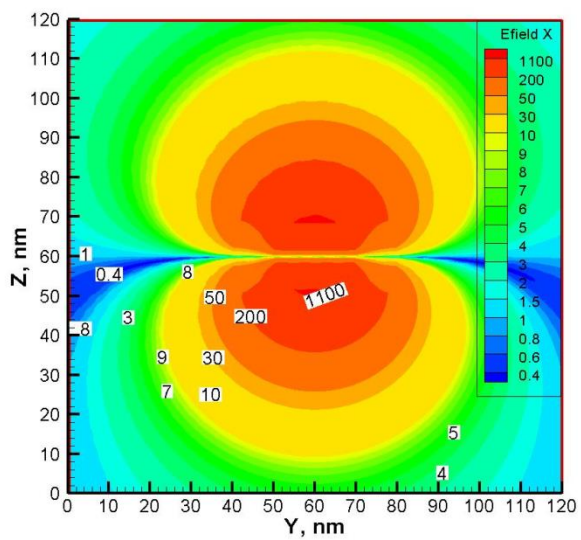

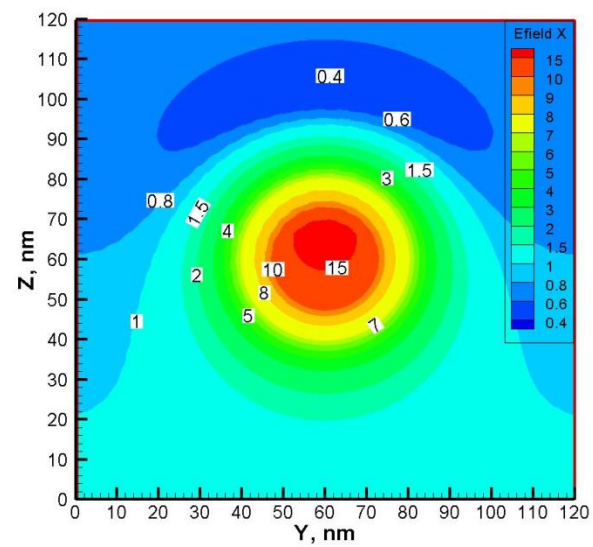

Lightweight Fluorescence Down-Converting Concentrators (1 kW per kg)

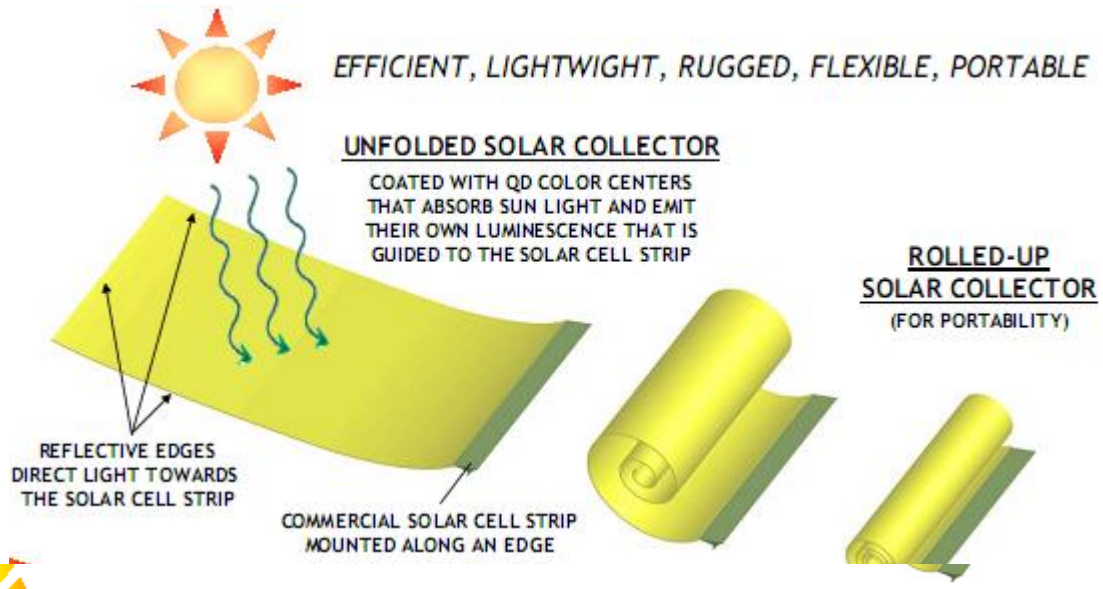

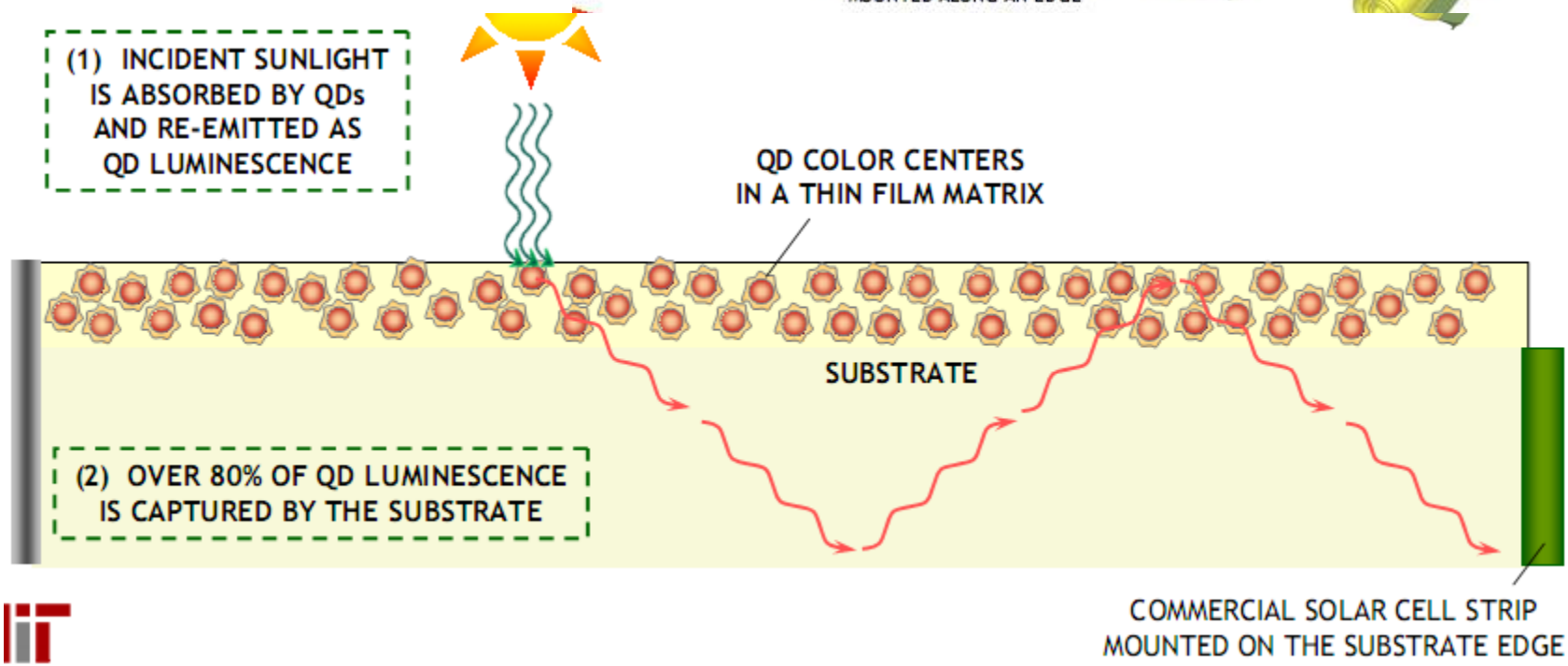

Summary: the key advantages of QDs

Size quantization allows to control the band gap energy and, therefore, to collect the major part of the solar spectrum.

- Multi-Exciton Generation produced by one photon.
- Overal gain of the current by means of “hot” electrons extraction system.
- QDs increase the efficiency of solar cells.
- Buildings blocks for nanotechology.